The Ablation Performance of Phenolic and Carbon Matrix Composites Under the Free Jet Conditions of Hybrid Propellant Rocket

by

Serhan Enes Kalmış

A Dissertation Submitted to the
Graduate School of Sciences & Engineering
in Partial Fulfillment of the Requirements for
the Degree of

Master of Science

in

Mechanical Engineering

December 31, 2023

The Ablation Performance of Phenolic and Carbon Matrix Composites Under the Free Jet Conditions of Hybrid Propellant Rocket

Koç University

Graduate School of Science & Engineering

This is to certify that I have examined this copy of a master's thesis by

Serhan Enes Kalmış

and have found that it is complete and satisfactory in all respects,
and that any and all revisions required by the final
examining committee have been made.

Committee Members:

_____

Assoc. Prof. M. Arif Karabeyoğlu (Advisor)

_____

Prof. Metin Muradoğlu

_____

Prof. Onur Tunçer

Date: 31 December 2023

To my wife and family

ABSTRACT

The Ablation Performance of Phenolic and Carbon Matrix Composites Under the Free Jet Conditions of Hybrid Propellant Rocket

Serhan Enes Kalmış

Master of Science in Mechanical Engineering

December 31, 2023

Ablative composite materials are commonly preferred in rocket nozzle regions where high temperature durability and shock resistance are required. In hybrid rocket motor applications, these materials are exposed directly to the hot gas products formed by the combustion reaction of fuel and oxidizer. Accordingly, ablation testing under the free-jet of lab-scale hybrid rocket motor would be flight-like simulation for the application of these materials in hybrid propellant rockets. As observed in the literature; Polymer Matrix Composites (PMCs), reinforced with silica and carbon fibers, can withstand short-term exposure to hot gases of combustion, whereas Ceramic Matrix Composites (CMCs), as Carbon/Carbon (C/C), exhibit exceptional durability without significant recession in similar conditions. In this work, chopped and 2D fabric reinforced phenolic matrix PMCs, and C/Cs were tested under the hot exhaust of paraffin fuel and gaseous oxidizer-based lab-scale hybrid rocket for 7 sec. In order to observe the oxygen-to-fuel ratio (O/F) effect on the ablation performances, each sample was tested in both oxygen-rich and fuel-rich firing conditions. Surface temperatures of samples were measured by two-colour IR pyrometer, also ablation rates were determined from the mass loss of samples. Test results show that phenolic matrix and C/C composites are significantly ablated by fiber-matrix debonding. Heat treatment of C/C samples in 1500 °C increased the ablation resistance by enhancing fiber-matrix bonding against hot gas exposure. For both phenolic matrix and C/C composite samples, chopped fiber reinforced samples propose better ablation resistance than 2D reinforcement. The variety of samples provides clear understanding about the ablation mechanisms of composite materials, specifically in the hybrid rocket applications.

ÖZETÇE

Fenolik ve Karbon Matrisli Kompozitlerin Hibrit Yakıtlı Roket Serbest Jeti Altındaki Ablatif Performansı

Serhan Enes Kalmış

Makine Mühendisliği, Yüksek Lisans

31 Aralık, 2023

Yüksek sıcaklık dayanımı ve şok direnci gerektiren roket nozülü bölgelerinde yaygın olarak ablatif kompozit malzemeler tercih edilir. Hibrit roket uygulamalarında ise bu malzemeler doğrudan yakıt ve oksitleyicinin yanma reaksiyonu sonucu ortaya çıkan sıcak gaza maruz kalırlar. Laboratuvar ölçekli hibrit yakıtlı roket motorunun serbest jeti altında yapılacak olan ablasyon testleri, bu malzemelerin hibrit yakıtlı roket uygulamalarındaki uçuş benzeri bir simülasyonu olacaktır. Literatürdeki benzer koşullar göz önüne alındığında, silika ve karbon elyaf takviyeli Polimer Matrisli Kompozitler kısa süreli sıcak gaz maruziyetine dayanabiliyorken Karbon/Karbon gibi Seramik Matrisli Kompozitler ciddi bir ablasyona uğramadan dayanıklılık gösterebilirler. Bu çalışmada fenolik reçine esaslı kırpılmış ve iki boyutlu elyaf takviyeli Polimer Matris Kompozitler ile Karbon/Karbon Kompozitler, parafin yakıt ve gaz oksijen oksitleyici içerikli laboratuvar ölçekli hibrit roketin 7 saniye süreli sıcak yanma gazına maruz bırakılmıştır. Yanmadaki oksijen-yakıt oranının ablasyon performansı üzerindeki etkisini gözlemlemek için her numune tipi oksijen zengin ve yakıt zengin ateşleme koşullarında test edilmiştir. Kızılötesi pirometre aracılığıyla numunelerin test esnasındaki yüzey sıcakları ölçülmüştür, ek olarak numunelerin kütle kayıpları ile ablasyon süratleri hesaplanmıştır. Test sonuçlarına göre fenolik matrisli kompozitlerin ve Karbon/Karbon kompozitlerin fiber-matris ayrılması nedeniyle ablasyona uğramakta olduğu gözlemlenmiştir. 1500 °C ısıl işlem uygulanması sonrasında Karbon/Karbon numunelerin sıcak gaz maruziyetine karşı ablasyon direncinin arttığı görülmüştür. Hem fenolik matrisli kompozitler hem de Karbon/Karbon kompozitler açısından kırpılmış elyaf takviyeli numuneler, iki boyutlu elyaf takviyesinden daha yüksek ablasyon direnci sağlamıştır. Numune çeşitliliği sayesinde, kompozit malzemelerin hibrit yakıtlı roket uygulamalarındaki ablasyon mekanizmaları hakkında net bir anlayış sağlanmaktadır.

ACKNOWLEDGEMENTS

I would like to express my deepest gratitude to my supervisor Assoc. Prof. Arif Karabeyoğlu whose admirable expertise, continuous support and precious feedback have played invaluable role in this study. Also, tangible results couldn't be exhibited without the fund, test facilities, and the essential tools provided by DeltaV Space Technologies.

Special appreciation to Dr. Mustafa Baysal, my mentor, whose deep knowledge and guidance have been instrumental in shaping this research. I am grateful for the opportunity to learn from his wealthy experience and constant excellence pursuit.

I would like to acknowledge the valuable contributions of Büşra Kahraman and Mehmet Kemal Ergin, who enriched the study by their experiences and companionship during the operations conducted for this research.

Additionally, I am thankful to DeltaV technicians Samet Bursa and Ahmet Başoğlu for their assistance during the tailoring manufacturing and testing operations. Their exceptional hands-on skills have been crucial to the practical aspects of this study.

To my family, your unhesitating belief and support were constant source of my motivation.

Finally, I want to share my heartfelt gratitude to my wife and life partner, Simge Aydınalev Kalmış. Her understanding and encouragement have been pillars that give me the strength to not only overcome academic challenges, but also in every aspect of my life.

Table of Contents

LIST OF TABLES

LIST OF FIGURES

NOMENCLATURE

A	Area
A_j	Pre-exponential Factor of Oxidation Reaction Species
β	Non-dimensional Blowing Parameter
c^*	Characteristic Velocity
C_F	Thrust Coefficient
E_j	Activation Energy
F	Thrust Force
g_0	Standard Gravity
G	Mass Flow Rate of Propellant
I_{sp}	Specific Impulse
I_t	Total Impulse
j	Oxidation Reaction Rate
k_j	Arrhenius Reaction Constant
$\dot{m}$	Mass Flow Rate
M	Molecular Weight
p	Partial Pressure
P	Pressure
$\dot{r}$	Regression Rate
R	Specific Gas Constant
$\dot{s}$	Ablation Rate
t	Time
T	Temperature
T_g	Glass Transition Temperature
v	Velocity
V_f	Fiber Volume Fraction
V_r	Resin Volume Fraction
x	Position
α_i	Sticking Coefficient
β	Non-dimensional Blowing Parameter
μ	Viscosity

ρ	Density

Subscripts

i	Species
e	Exit
a	Ambient
t	Throat
ox	Oxidizer
f	Fuel
p	Port

ABBREVIATIONS

AR	Area Ratio
BMI	Bismaleimide
CEA	Chemical Equilibrium with Applications
CFRP	Carbon Fiber Reinforced Polymer
CMC	Ceramic Matrix Composite
CVI	Chemical Vapor Infiltration
FR	Fuel Rich
GOX	Gaseous Oxygen
HDPE	High Density Polyethylene
HTPB	Hydroxyl-terminated Polybutadiene
IPA	Isopyopyl Alcohol
LOX	Liquid Oxygen
OR	Oxygen Rich
PAN	Polyacrylonitrile
PMC	Polymer Matrix Composite
SRM	Sounding Rocket Motor
TGA	Thermogravimetric Analysis

Chapter 1:
INTRODUCTION

The nozzle region in rocket motors is exposed to extremely high temperatures and pressures, since the hot combustion products of motor are pressurized and expanded in there. High temperature resistance, thermal stability, and shock resistance of composite materials make them suitable for nozzle region material selection, especially silica and carbon reinforced polymer matrix composites or ceramic matrix composites. Additionally, the excessive heat flux of combustion products could be dissipated by sacrificial ablation of composite materials in high temperatures, therefore nozzle region could be thermally protected from excessive heating for a particular time. Graphite and refractory metals are commonly used in nozzle regions too; however, ablative composites' fiber reinforced structure offers better fracture toughness than graphite in addition to its lighter weight than refractory metals.

Specifically in hybrid rocket motors, the temperature of nozzle regions exceeds 2000 °C under the flow of oxidative hot gases such as water vapor (H_2O), carbon monoxide (CO), and carbon dioxide (CO_2). Even if the Ceramic Matrix Composites (CMCs) as Carbon/Carbon (C/C) and Carbon/Carbon-Silicon Carbide (C/C-SiC) could withstand this condition, the duration of firing is critical to prevent overdesigned material selection. In ablative Polmer Matrix Composites (PMCs), high temperature resistant silica or carbon fiber reinforcement is supported with charring matrix, such as phenolic. Charred matrix forms a protective carbon layer by decomposing under the heat without oxidizing gases. Polymer matrix provides short term durability under the high temperature conditions of rocket nozzles, even if their continuous operating temperature is below 350-400 °C. On the other hand, C/Cs include previously carbonized matrix rather than in-situ carbonization as in polymer matrices. As the stiffness of carbon is maintained its high thermal stability in temperatures exceeding 1500 °C, C/Cs provide long term durability. Although carbon-based composites preserve their stiffness in high temperatures, they are vulnerable to oxidation above 450 °C which could lead decrease in nozzle efficiency due to faster ablation. While silicon infiltration to C/C is suitable alternative for oxidation protection by forming SiC that proposes decomposition above 2300 °C in CMCs , silica

fiber reinforced PMCs provide short term durability against high temperature oxidative conditions of rockets as it melts above 1700 °C and protects underlying layers by melting.

If an ablative composite material is designed for hybrid rocket nozzle region, it has to be qualified for pressurized oxidizing hot gas environment, higher than 2000 °C with high flow rates. In general, high temperature composite ablatives are tested in costly and sophisticated arc jet facilities, that could apply high heat flow by using air and nitrogen. On the other hand, arc jet testing could not provide pressurized environment as in nozzle region. Oxy-acetylene torch is another common ablation testing heat sources, however it applies heat flux up to 80 kW/m^2 with low pressure, while typical hybrid rocket nozzle works in the range of 5 to 15 MW/m^2 [Savino et al., 2017]. In recent years, high temperature ablative materials have started to be tested under the free jet of lab-scale rocket motors. The gas composition, temperature, heat flux and pressure environment of free jet tests are similar with the nozzle environment; since the free jet includes pressurized combustion products of rocket. Therefore, ablation testing under the free jet of lab-scale rocket motor proposes cost-effective flight like testing for the nozzle material selection. Additionally, free jet focused on the ablative composite sample applies impact which is mechanically tougher than pressure of combustion gas acts on the nozzle. Free jet test with rocket motor also could be designed by changing the combustion parameters and nozzle geometries to satisfy flight-like flow rate, heat flux, gas composition and pressure parameters.

A paraffin-based hybrid rocket motor with GOX oxidizer was used as free jet source to test ablative performance of phenolic and carbon matrix composites. The processing of ablative composites and ablation mechanisms of their constituents were studied in order to provide better understanding of composite selection for ablation applications. Samples were tested under the free jet of fuel and oxidizer rich hybrid rocket motor configuration. Based on the surface temperature and mass ablation rates of samples; ablation performances of samples were assessed.

Chapter 2:
LITERATURE REVIEW

2.1 Ablative Materials

2.1.1 Overview

High temperature composites have developed from the need of mechanically and thermally durable lightweight structural aerospace systems such as rockets and jet engines. Since glass fibers were available before 1960s and carbon fibers have started to be produced in 1960s, both type of fibers became the main interest in specific high temperature composites. Even if fibers such as alumina and boron fibers were developed for the same need, they were not mechanically sufficient in addition to their costly productions. For maintaining stable operations in high temperature, high temperature stiffness was critical requirement for fiber selection. While glass fibers were strong, they can't perform stiffness in elevated temperatures as they soften after 850°C. Carbon fibers preserve their stiffness in temperatures exceeding 1500 °C with low thermal expansion which is critical to handle thermal mismatch in thermal shocks [Meetham et al., 2001]. Since glass and carbon fibers had relative low cost of manufacturing and mechanical capabilities in elevated temperatures, they became the main focus in high temperature applications such as nozzle parts and heat shields.

The matrix of ablative composites has to resist high temperature as well, while preserving structural strength to maintain integrity of fiber reinforcement. Since the considerable heat removal is desirable under high heat flux, insulative characteristics such as large heat capacity with low conductivity and superior heat of ablation are favorable in matrices. Epoxy and phenolic resins have commonly used from 1950s due to their ablative properties. Teflon has superior ablative properties too; however the manufacturing of Teflon as composite matrix is unpractical. Phenolic resin was distinguished from other polymer matrices by its charring behavior. Virgin layer of phenolic is pyrolyzed and lefts carbon residue by releasing organic volatiles under the heat flux exposure, that protects the underlying structural layers from direct hot gas exposure. On the other hand, carbon is vulnerable to oxidizing gases above 450°C

therefore, direct hot gas exposure of phenolic or carbon is not preferable for nozzles in long duration firings.

After the development of C/C composites in 1950s, ceramic matrix composites had become the main interest in rocket nozzle applications. C/Cs perform superior mechanical properties than monolithic graphite by their improved toughness, tailorable fiber reinforced architecture and defect tolerance. Although they are vulnerable to oxidative gases, various matrices had tried to be implemented within carbon fiber reinforcement such as glass and silicon matrices. Since both glass and silicon react with carbon by forming Silicon Carbide (SiC) having high temperature oxidation resistance, SiC matrices and SiC fibers had taken part in CMCs. SiC formation around the carbon tows are quite efficient coating for oxidation resistance of carbons, hence various techniques have developed until today for manufacturing C/C-SiC and C/SiC composites.

CMCs have been designing mainly to resist the hypersonic hot gas exposure of certain components in rockets such as nozzles and high Mach number re-entering systems. Nevertheless, selecting the material by considering the limits of mission is important to prevent overdesigning subcomponents. While heatshields of rockets expose to light-density air with high speed, hybrid rocket nozzles have to resist oxidizer rich hot gas for stable firings or hybrid rocket injector has to be protected from relatively cold oxidizer. For example, phenolic impregnated silica felt was used for heat shielding underneath CFRP structure in Ariane 5 while C/C was preferred as nozzle throat material [Ariane-5, 2001]. Ariane 5 was aluminum containing solid propellant rocket that has lower oxidizing potential than hybrid rockets, that is C/Cs may not resist oxidizing combustion environment of hybrid propellant. Accordingly, ablative materials have to be designed with respect to operation conditions and ablation rate limits, which are directly related to ablation mechanisms of materials. Moreover, there could be specific ablation mechanism preference related to operation of subcomponents. Melting ablation is favorable in high melting point materials ,such as silica; since they dissipate and carry away heat in re-entries with their high heat capacity. On the contrary, melting behavior is not suitable for structural parts because of structural integrity collapses after the melting point is reached. Gasification would be better under intense heat flux exposure by limiting the ablation with surface, rather than affecting underlying layers providing structural strength.

2.1.2 Ablation Mechanisms

High heat flux is a critical factor as it affects the mechanical performance of components in flights. In order to maintain operation nominally, these components have to be protected from the excessive heating. Even if active cooling of parts is an effective method by removing heat with a cooling fluid, it brings extra weight with its subcomponents such as pump systems. The high heat flux exposure could be also lowered by transferring heat with conductive materials and sacrificial materials with high ablation enthalpy which is called passive cooling. As the flights have a certain duration to complete, passive cooling by using ablative materials is generally favorable rather than adding more weight with active cooling systems. Ablation behavior of flight components has to be simulated and tested in order to estimate ablation rate in flight operations.

Ablation mechanism is characterized according to the ablative material in addition to temperature, pressure, and gas species within ablative environment. While polymer matrix ablative composites are generally classified as pyrolyzable and non-pyrolyzable, CMCs cannot be pyrolyzed anymore. Therefore, further classification is required for defining ablation mechanism of non-pyrolyzable materials. Silica and carbon fibers are both non-pyrolyzable, however silica ablates by forming melt layer on the surface while carbon is oxidized within nozzle conditions. The common ablation mechanisms of composite ablatives are pyrolysis, oxidation, melting, vaporization, and sublimation.

2.1.2.1 Pyrolysis

The matrix of polymer composites undergoes pyrolysis by dissipating heat endothermically. The crosslinked aromatic rings of matrix are decomposed into char (carbon) residue by releasing organic volatiles above 250-300°C in the absence of oxidative gases. Porous char structure lowers the heat conduction through underneath virgin layers, while the releasing volatiles cool down the area and form thermal barrier against combustion species near the surface. The pressurization of pyrolysis products could induce delamination as well, as the charred matrix is still bonded to fiber reinforcement [Rallini et al., 2019].

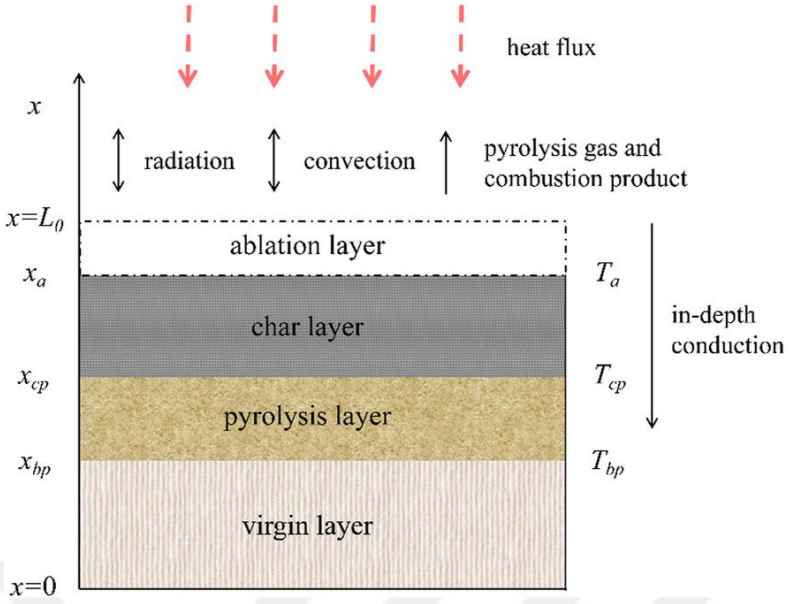

Figure 2.1: The Ablation Phenomena of Pyrolyzable Polymeric Ablatives [Xiao et al., 2021]

Hot pressurized gas ablates the charred layer by thermochemical ablation and mechanical erosion. While high temperature oxidative gases react with char layer, the surface exposes also to shear and pressure loads of flowing gas. Pyrolyzed layer has to resist as long as possible to protect underlying virgin layers. Strongly bonded tough and dense char layer perform better durability, therefore high char yielding polymers are favorable in ablative materials. As the surface is tougher and further char residue is available for heat consumption by chemical reactions, the ablation rate of the material will be lowered. Additionally, the amount of volatile release decreases in the high char yield materials, which contributes to lower the delamination and matrix crack risks. Phenolic, polyimide and bismaleimide (BMI) resins are commonly used as high char yielding ablative composites. Even if polyimide and BMI leave more char residue, phenolic is advantageous with lower cost, processing convenience and market availability [Schmidt, 1969].

Pyrolysis is completed up to 1000 °C in the oxygen free environment. Three steps of reactions could be identified to explain the conversion of phenol monomers to glassy carbon during pyrolysis. Steps are defined according to certain temperature-based decomposition regimes during the pyrolysis [Duffa, 2013].

1) Cured phenolic is depolymerized into phenol monomers, moreover methylene bridges react with free hydroxide (-OH) to form water vapor between 600 K and 800 K.
2) Side groups of phenol monomers react with each other, and release hydrogen (H_2), carbon monoxide (CO) and methane (CH_4) molecules, while aromatic rings are linked between 700 K and 1100K.
3) Between 900 K and 1200 K, remaining aromatic groups abstract hydrogen to form an amorphous, non-ordered glassy carbon structure above 600°C [Duffa, 2013].

Temperature (K)	Reaction	Type
$600 < T < 800$	$R_{CH_2} \rightarrow R(CH_3)_n$ $2R_{CH_2} \rightarrow R_{CH} + H_2O$	Depolymerization condensation $(-CH_2-) + (-OH)$
$700 < T < 1100$	$2R_{CH_2} \rightarrow R_O + H_2O$ $R_O \rightarrow R + O$ $R_{CH_2} + O \rightarrow R + CO + H_2$ $R_{CH_2} + H_2O \rightarrow R + CO + 2H_2$ $R_{CH_2} + H_2 \rightarrow R + CH_4$ $R_{CH} \rightarrow R + H_2$	Condensation $(-OH) + (-OH)$ Reaction $(-CH_2-) + H_2O$ Reaction $(-CH_2-) + H_2$
$T > 900$	$R \rightarrow R_d + H_2$	Hydrogen abstraction

Figure 2.2: Phenolic Resin Pyrolysis Reaction Regime [Duffa, 2013]

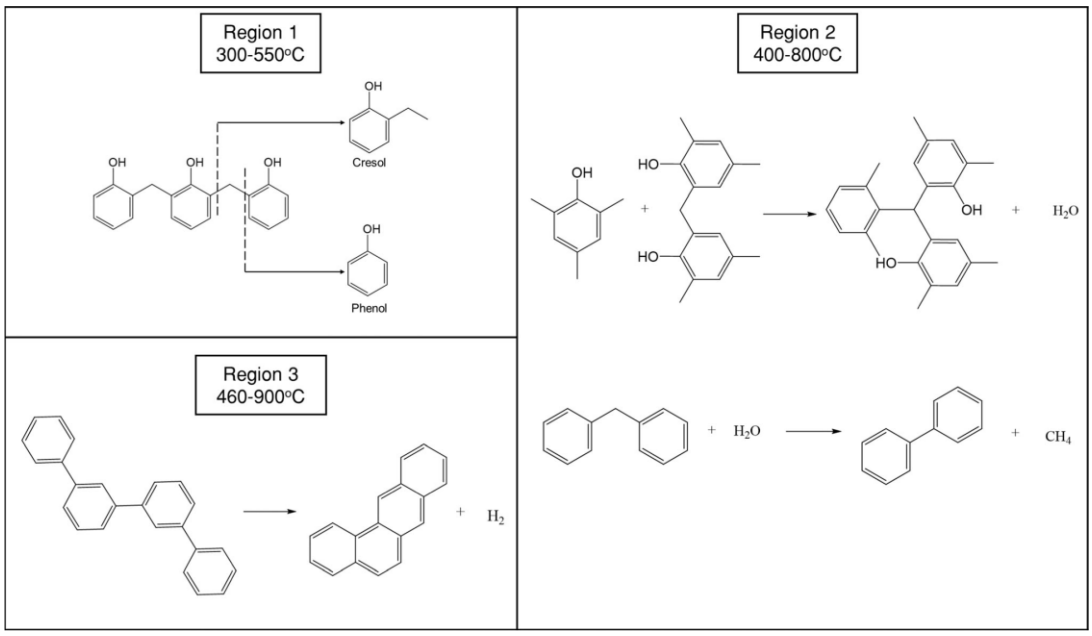

Figure 2.3: Reactions of Partially Pyrolyzed Phenolic Resin [Trick et al., 1997]

Apart from direct ablation application, the decomposition regimes of pyrolysis reactions are critical for C/C composite manufacturing. Carbon fiber reinforced high char yield polymers are pyrolyzed to obtain carbon matrix, in the atmospheric controlled pyrolysis furnaces. By considering the decomposition regime of phenolic which includes extraction of various organic products, the heating rate of pyrolysis has to be designed. Lower heating rate provides controlled release of pyrolysis products, hereby structural damages within C/C products are reduced, such as delamination and matrix cracks.

2.1.2.2 Oxidation

Understanding and estimating the ablation behavior of carbon is critical, because of the common usage of charring polymers, C/Cs and graphite in ablative materials. Hot gas species oxidize these materials thermochemically. Even if carbon can be consumed by nitridation and sublimation as well, they are neglected in oxidative hot gas environment due to high portion of oxidation reaction. Oxidative combustion products react and remove the carbon atoms in the concept of active wall site [Duffa, 2013]. Therefore, graphitization is favorable in ablation applications in order to stabilize carbon microstructure by decreasing active sites. On the other hand, oxidation reaction constants have assumed same in the ablation models whether it is graphitized or pyrolyzed [Turchi, 2013]. In Table 2.1, reaction constants are defined for the oxidation of solid carbon (C_s) with OH, H_2O, CO_2 and O_2 species.

Table 2.1: Rate Constants for the Carbon Oxidation Reaction [Bradley et al., 1985]

	Reaction Rate Constants				Mass Ablation Rate
Reaction	j	A_j	E_j $(kJ.mole^{-1})$	B	$\dot{m}_i$ $(kg.m^{-2}.s^{-1})$
$C_s + OH \rightarrow CO + H$	1	361 $kg.K^{1/2}.m^{-2}.s^{-1}.atm^{-1}$	0	-0.5	$\dot{m}_1 = k_1.p_{OH}$
$C_s + H_2O \rightarrow CO + H_2$	2	$4.8\ x\ 10^5$ $kg.m^{-2}.s^{-1}.atm^{-0.5}$	288	0	$\dot{m}_2 = k_2.p_{H_2O}^{0.5}$
$C_s + CO_2 \rightarrow 2CO$	3	$9\ x\ 10^3$ $kg.m^{-2}.s^{-1}.atm^{-0.5}$	285	0	$\dot{m}_3 = k_3.p_{CO_2}^{0.5}$
$C_s + \frac{1}{2}O_2 \rightarrow 2CO$	4	2400 $kg.m^{-2}.s^{-1}.atm^{-1}$	125.6	0	$\dot{m}_4 = \frac{k_4.p_{O_2}.Y}{1 + k_5.p_{O_2}} + k_6.p_{O_2}.(1-Y)$ for $Y = \left[1 + \frac{k_7}{k_6.p_{O_2}}\right]^{-1}$
	5	21.3 atm^{-1}	-17.17	0	
	6	0.535 $kg.m^{-2}.s^{-1}.atm^{-1}$	63.64	0	
	7	$18.1\ x\ 10^6$ $kg.m^{-2}.s^{-1}$	406.1	0	

Oxidation reaction rates j are described in Equation 2.1 by Arrhenius law for the oxidizing species i. A_j represents the pre-exponential factor of species , T is the wall temperature, E_j is the activation energy, R is the specific gas constant, and p is partial pressure. The partial pressure is determined according to the mole fraction of exhaust combustion products and total pressure on ablation surface, specifically for the nozzle and free jet test ablative materials. By multiplying the Arrhenius reaction constants with partial pressure p (in the power of reaction order) mass ablation rate is obtained.

$$k_j = A_i.T^B.\exp\left(-\frac{E_i}{R.T}\right) \tag{2.1}$$

Total ablation is the sum of mass ablation rates for each oxidative species as in Equation 2.2. Mechanical erosion is neglected, since the thermochemical ablation behavior is the main factor that drives the surface recession and carbon is assumed strong enough to resist mechanical erosion in high temperatures.

$$\dot{m}_{total} = \dot{m}_1 + \dot{m}_2 + \dot{m}_3 + \dot{m}_4 \tag{2.2}$$

2.1.2.3 Melting & Vaporization

Melting ablative materials sink the heat from hot gas until the surface temperature reaches to melting point. Thereafter, the liquified layer blows off or drips from the surface. New solid surface is emerged, and the material recesses steadily by the formation of particular temperature profile [Natali et al., 2012]. The excessive heat is removed from the material by decomposition and vaporization of melted material. Additionally, melting and vaporization of material thicken the surface boundary layer, which lower the convective heat transfer to underlying virgin layers [Favaloro, 2000].

Carbides and oxides are highly preferred because of their high temperature melting point, heat capacity and oxidation resistance [Natali et al., 2012]. Silica fiber reinforced polymer composites are prevalent in short duration firings which melts above 1700°C. However, it softens close to melting temperature by risking structural performance. For longer duration firings, Silicon Carbide (SiC) could endure 1500°C continuously even in oxygen rich environments with good erosion resistance, also generally used as throat insert in nozzles. SiC ablates both by oxidation and melting, however silica fiber melts directly. Specifically, SiC is preferred in ultra-high temperature applications, while Silica reinforced phenolic polymeric composites are widely used in nozzle regions due to its cost-effective high temperature resistance.

Silica-Phenolic (SP) composites dissipate most of the heat by mass loss. As the silica reaches melting temperature, surface is cooled down due to the removal of silica's blowing and vaporization. Therefore, the surface of material is assumed isothermal at the melting temperature in ablation modelling [Turchi, 2013]. Surface recession is also affected by shear force and viscosity of melt material in addition to thermal properties of SP composite. It is desirable to dissipate heat even after the melting by vaporization and chemical reaction of silica by using non-blowing droplets. High melt viscosity and low shear force contribute further heat dissipations, also reduce recession rate [Natali et al., 2012].

Although the pyrolyzed matrix oxidizes after 400°C, melt silica layer blocks oxidation of matrix by the hot gas flow. As the carbon could resist up to sublimation temperature 3000°C, which is quite higher than melting point of silica; the surface cooling effect is lowered by the melt silica blockage [Natali et al., 2012]. That is, surface temperature could reach more than melting point of silica if the liquified fiber does not

sweep from the surface suddenly. On the other hand, carbon's strength in elevated temperatures is negligible under the oxidative flow. It could be assumed that removal of carbon occurs within the blowing of melt silica, and the recession rate is driven by silica's mass loss. Eventually, the main recession factor of SP composite is silica's blowing that is driven by surface temperature, shear force and melt viscosity [Natali et al., 2012].

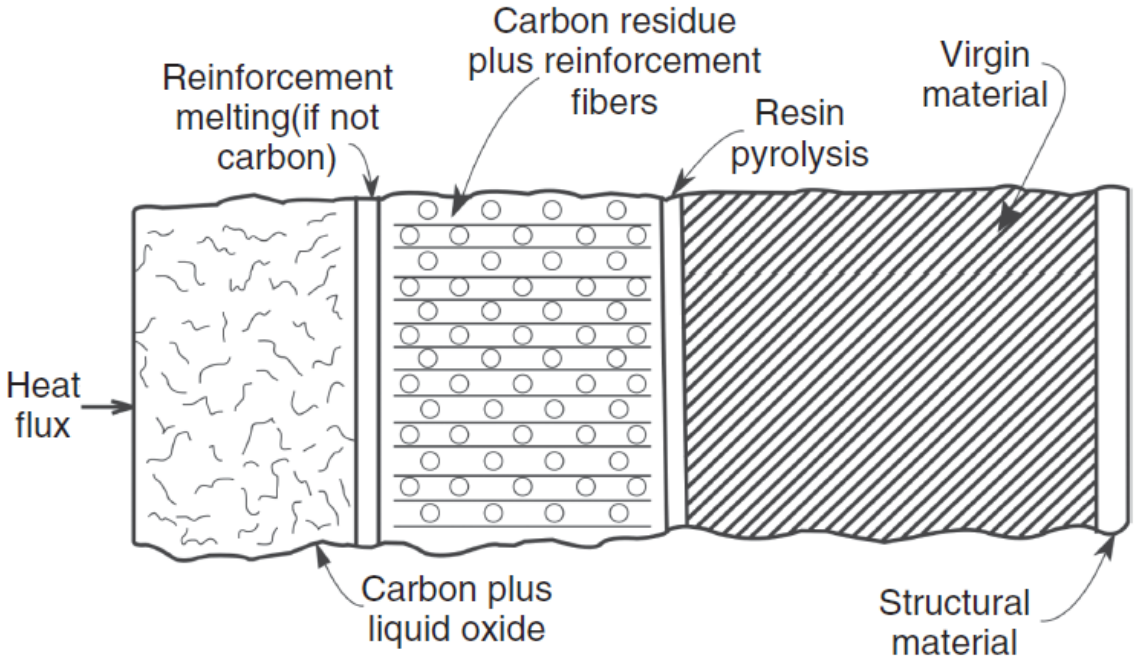

Figure 2.4: The Ablation Schematic of Silica Phenolic Polymeric Composite [Natali et al., 2012]

2.1.2.4 Sublimation

Carbon based ablative materials begin to sublimate above 3500 K in atmospheric pressure. Especially in high enthalpy flows such as entry and re-entry, the surface temperature of thermal protection shields could reach or exceed sublimation temperature. The solid carbon change phases directly to gas state. Unlike thermochemical reaction and melting, recession rate could induce sudden shape changes [Martin, 2013]. Therefore it is critical to design a controlled ablation for the flight to prevent catastrophic failures in high-enthalpy flows. In order to prevent oxidation of carbon by the atmospheric species, thin coatings are applied to carbon based ablative material [Favaloro, 2000].

Depending on the contribution of various ablation mechanisms to recession, the main ablation regimes of carbonaceous material could change. While oxidation reaction is the overall mass loss for low temperatures, diffusion of oxidative species become critical in

higher temperatures because of the increase in active sites on carbon structure. When the surface reaches sublimation temperature, mass loss rate by oxidation is lowered and sublimation drives the largest recession portion [Martin, 2013]. Sublimation rate is also affected by stagnation pressure on the surface. Since the solid to gas phase transition occurs by vapor pressure difference, higher stagnation pressure would lower the mass loss rate by sublimation [Turchi et al., 2019]. Accordingly, sublimation is not valid phenomena for nozzle inserts of Sounding Rocket Motors (SRM), since the temperature is lower than sublimation point in addition to exposure to high static pressure [Onay, 2020].

During the sublimation of carbon, linear and low weight carbon molecules are released mostly, such as C, C_2 and C_3. Mass loss in sublimation could be described by Knudsen-Langmuir Law [Duffa, 2013].

$$\dot{m}_i = \alpha_i \left(\frac{\mathrm{M}_{C_i}}{2.\pi.R.T} \right)^{\frac{1}{2}} (p_{C_{i_{eq}}} - p_{C_i}) \tag{2.3}$$

Sticking coefficient α_i is obtained by experimental results determined for each species, depending on the temperature [Duffa, 2013].

Table 2.2: Sticking Coefficients for Carbon Sublimation [Duffa, 2013]

Species	α_i (2500K)	α_i (2450K)	α_i (2700K) (Base Plane)
C	0.14-0.23	0.37	0.24
C_2	0.26-0.38	0.34	0.50
C_3	0.03-0.04	0.08	0.023

2.1.3 Processing

In the aerospace industry, composite materials are designed by considering mechanical, corrosive, thermal and weight requirements of specific structural or thermal parts. These parts are composed of fiber reinforcement embedded in polymer or ceramic matrix. The reinforcement might be long or short fiber surrounded by various types of matrices such as thermoset resin, rubber, or ceramic. Even if the composite raw material production volume is higher compared to previous years, manufacturing processes couldn't expand accordingly due to highly tailoring procedures [Peters, 1998]. Since composite parts are manufactured for specific structures under different mechanical and thermal load directionalities, they are hard to implement in mass production, such as metals, at least for now. In Figure 2.4, composite materials are classified according to reinforcement types.

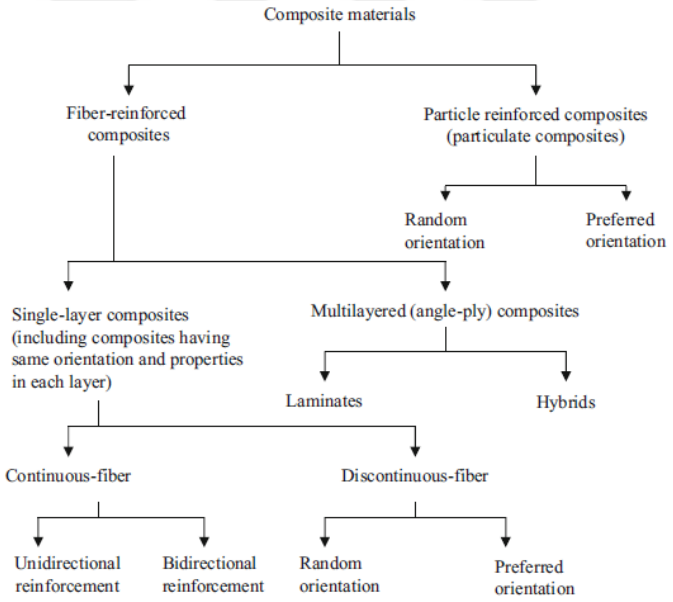

Figure 2.5: Composite Material Classification for Various Reinforcement Types [Sharma et al., 2017]

Polymer ablative composites could perform comparable mechanical properties with metals and conventional composites, in addition to their thermal durability. They are also largely fabricated for precursor (starting polymeric material) of C/Cs, due to the knowledge in manufacturing techniques and carbon leaving resins [Sharma et al., 2017]. Especially in rockets, thick lamination, complex and bulk shapes are prevalent, since

ablative composites are used in motor insulation liners, nozzle regions, nose caps and heat shields. High temperature polymer resins are highly viscous and rich by volatile, also they are cured in high temperatures compared to traditional resins. In order to reduce porosity and impregnate fibers well, high pressure and temperature is required during curing [Schmidt, 1969]. Accordingly, hot press, compression molding, resin transfer molding, filament winding, and autoclave processes are commonly preferred. Operational costs of these processes are high due to tooling requirement, gas consumption, and disposable equipment. Since resins of ablative applications are toxic by volatile that brings infrastructural requirements too, such as ventilation and atmospheric conditioning [Sharma et al, 2017].

Even if ceramics are inherently brittle and vulnerable to thermal shocks, embedding them into fiber reinforcement provides tough structures. SiC and C fiber reinforced ceramic matrices are highly preferred in the nozzle regions of rockets. The impregnation of CMCs is generally performed by polymer precursor infiltration, melt infiltration in high temperatures and chemical phase infiltration. Silicon and carbon both have polymer precursors such as polycarbosilane and phenolic resin, which widely preferred in C and SiC based CMCs. During the heat treatment and pyrolysis of polymer precursors, organic products are released by leaving porosity within parts. Therefore, impregnation and pyrolysis cycles are required for densifying parts.

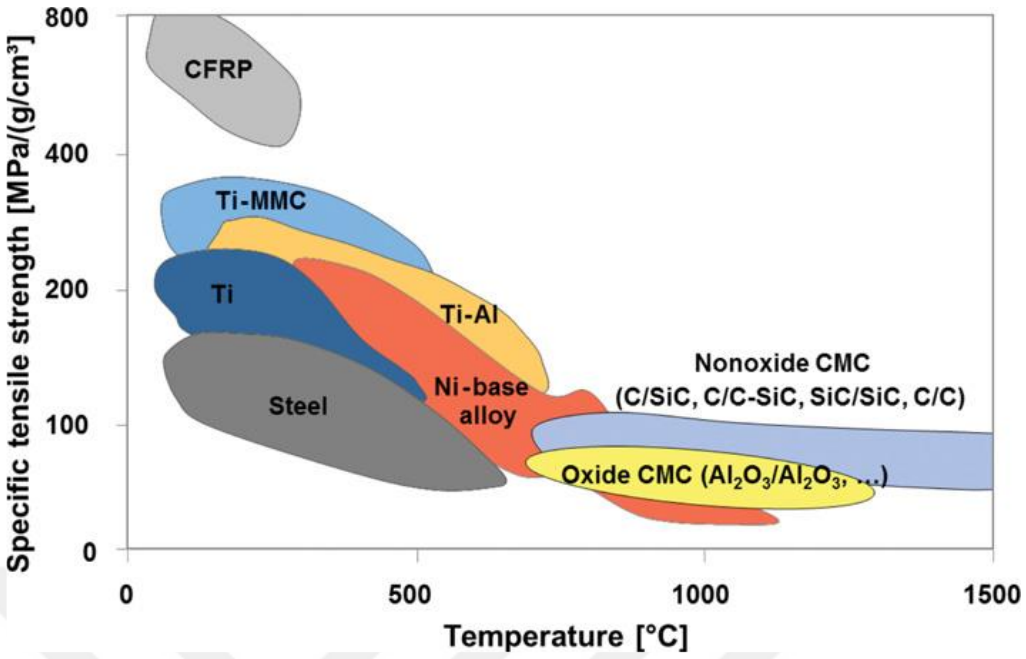

Figure 2.6: Specific Strength of Materials as a Function of Temperature [Bansal et al., 2014]

2.1.3.1 Polymer Matrix Composites

Polymers are practical to form matrix structures within fiber reinforcements. They are mechanically weaker than metals and serve in lower temperature ranges compared to metals. On the other hand, resins of polymer matrices are eligible in terms of processibility and handling for tailoring composite manufacturing. Due to the practical use of resins, PMCs could be manufactured by versatile impregnation and lamination techniques [Chawla, 2012]. Thermosets and thermoplastics are commonly used in PMCs. While thermoplastics soften by heating and harden in lowered temperature, thermosets harden by curing chemical reaction of monomers within resins [Chawla, 2012]. Polymer matrices of ablative applications have to serve beyond their glass transition temperatures T_g, whether it is thermoset or thermoplastic. Related studies shows that polymers involving aromatic units could perform higher mechanical properties and oxidation resistance in high temperatures [Peters, 1998].

Most of the resins used in ablation applications (phenolics, polyimides and bismaleimides) cured by condensation polymerization reaction, that extracts side products such as water. Additionally, monomers of aromatic resins (phenolics,

polyimides, bismaleimides) are highly viscous and resins have to dissolved within solvent for processability, therefore they are generally available with suitable solvent such as ethanol, methanol, or water. Solvents and side products have to be eliminated before complete hardening of resins, since they form voids in matrices. Consolidation pressure and vacuum evacuation are commonly applied on impregnated laminates to suppress formation and growth of voids [Chawla, 2012]. As many resins with aromatic content cure in high temperature and pressure; process consumables and tooling should resist to harsh curing conditions as well. Instead of commonly used nylon vacuum bags and polyester bleeders, which are suitable in epoxy, polyester, and vinyl ester curing; steel connectors, polyimide release films, and fiberglass bleeders are preferred in high temperature resin curing. Hence, curing operations of ablative polymeric matrices are costly. Even if processing conditions of high temperature resins are exhaustive compared to common resins, their manufacturing is cheaper than ceramic matrix composites.

Polymer matrix composites couldn't endure long-term high temperature oxidative firings. Accordingly, PMCs are designed in thick and bulk geometries in order to resist longer firings. Regardless of fiber reinforcements are continuous, discontinuous, or weaved, the manufacturing of thick composites requires well-controlled heating and pressure distribution that causes additional challenges to the curing high temperature resins. For longer term firings, CMCs are more suitable.

2.1.3.2 Ceramic Matrix Composites

Ceramic materials perform high stiffness and hardness, chemical inertness, and low conductivity in remarkably high temperatures, which make them convenient selection for rocket nozzle applications. They have higher melting point and strength-to-weight ratio than metal alloys. By their very high melting temperature, low thermal conductivity, and high heat capacity; ceramic materials can resist long-duration firings of rockets with low erosion rates. The limiting factor of ceramics is their terrible toughness. They couldn't exhibit plastic behavior under loading; thus flaws and voids could lead catastrophic failures. As the high melting temperatures of ceramics decrease processing convenience, manufacturing defects are hard to eliminate. Reinforcing ceramic materials by particulates, short and continuous fibers is efficient way to develop toughness and plasticity [Peters, 1998]. Glass, carbon, borides, oxides, and carbides are widely used in

CMCs as both reinforcements and matrices [Rana et al., 2016]. CMCs can be processed in powder, liquid, and vapor form.

In the powder form, composite design is determined, then constituents are selected according to mechanical, chemical, and thermal compatibility. Constituents are mixed homogenously by taking care of agglomeration, which depends on the interaction of powders, fibers, and binders within mixture. Depending on the facilities and composite design, packed powder phase constituents could be cold pressed and hot pressed. While cold pressing requires additional packing, binder removal, and sintering operations; hot pressing includes concurrent packing and sintering in elevated temperatures. During the heating, reaction, and cooling stages of processes; constituents within packed structure may exhibit thermal mismatch and chemical degradation due to thermal and chemical conditions [Sharma et al, 2017]. Additionally, sintering stages are critical because many cracks are associated with shrinkage in CMC processing.

Optimum mechanical performance of powder based ceramic mixtures couldn't be obtained by packing in high temperature and pressure. Resulting part in powder processing includes crack and flaws due to incompatibility of constituents during the processing in high temperature and pressure ranges. Near void-free composites could be manufactured by liquid infiltration of ceramic matrices in a single process. Just like liquid polymer or metal infiltration, melted ceramic could be infiltrated through reinforced preform and fill pores within composite until reaching full density. Disadvantageous of liquid infiltration is high melting temperature and viscosities of ceramics may lead to wettability problems. Moreover, high temperature melt infiltration can cause chemical reactions and thermal mismatches with fiber reinforcement. After optimizing the process, melt infiltration propose single step and fully densified matrix formation [Peters, 1998].

Fiber reinforcement could be impregnated by chemical vapor as well. In the chemical vapor infiltration (CVI) method, gaseous reactant is deposited onto reinforced preform, then decomposes within fiber reinforcements to yield ceramic matrix. Reinforced preform is kept in the decomposition temperature range of gaseous reactant, for example silane-hydrocarbon reactants form SiC in the range of 1000 °C–1400 °C. Since the matrix is formed rapidly in outer surface pores by infiltration, process has to be interrupted in order to reopen gas entrance by grinding surface. The final product usually has porosity content between 10% to 20%. Complex and near-net shape parts could be produced by CVI in addition to good mechanical properties. On the other hand, the process is slow and

expensive, also couldn't provide near void-free parts as liquid infiltration [Sharma et al, 2017].

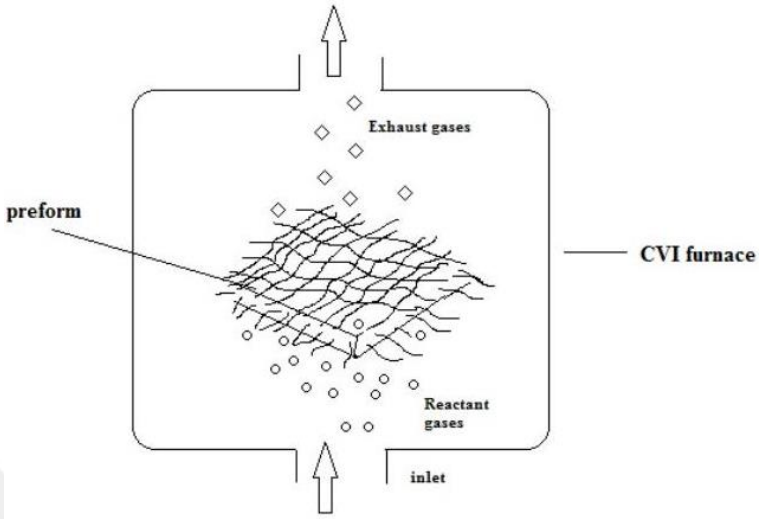

Figure 2.7: Schematic of Isothermal-CVI Process [Coltelli et al., 2019]

CMCs are quite favorable candidates for nozzle material selection except their inclination to catastrophic failures by low fracture toughness. Among oxides, glass, and boron fibers; carbon fibers are favorable in terms of preserving strength and stiffness in high temperature conditions. Additionally, carbon is eligible to obtain as matrix from charring polymers. Due to the familiarity of PMC processing in industry and low temperature processing ability of polymers, C/Cs are favorable in nozzle applications. Due to their oxidation vulnerability; carbon fibers and matrix have to be protected with coatings such as SiC and SiO_2.

Carbon-Carbon

Carbon materials perform high strength and stiffness in addition to their chemical and thermal stability in high temperature inert environments. In spite of common weak fracture toughness property of CMCs, C/Cs exhibit well fracture toughness and impact tolerance in elevated temperatures. Basically, C/Cs are composed of fibrous carbon reinforcement embedded in carbon matrix. Fiber and matrix could represent different types of carbon elements from carbon to graphite [Peters, 1998]. For example as fibers, carbon could be based on rayon, petroleum pitch or polyacrylonitrile (PAN), also the matrix might be derived from thermoplastic pitch, thermoset polymeric resin, or

hydrocarbon gases [Chawla, 2012]. Accordingly, constituent carbons could perform different thermal and mechanical properties in processing and applications.

Just like carbon-epoxy polymer composites, C/Cs are generic composite materials, that is manufacturing processes are not unique as other CMCs and mostly comply to state of art [Peters, 1998]. The main objective in C/C manufacturing is filling carbon fiber reinforcement with a precursor matrix that could be carbonized. There are two common methods to manufacture C/C composites; carbonization of thermosetting or thermoplastic precursor, and chemical vapor infiltration (CVI).

Thermoset carbon precursors are obtained by conventional techniques of PMC manufacturing [Chawla, 2012]. As stated in section 2.1.3.1, polymeric resins such as phenolic, polyimide, bismaleimide (BMI) leave carbon residue by eliminating volatile side products around 1000 °C inert atmosphere. Carbon precursor polymeric composites are manufactured by filament winding, hot press, autoclave curing; then carbonized to obtain carbon matrix. C/C parts are carbonized and re-infiltrated by resins multiple times until reaching desirable final density, since new emerging voids resultant of pyrolysis are filled by matrix. It is desirable to select high carbon yield polymeric precursors to minimize the number of densification cycles. Phenolic resins are widely used due to their availability and relatively high carbon yield [Chawla, 2012].

Pitch is thermoplastic material that is highly viscous and softens in high temperatures. Carbon fibers are impregnated by pitches under heat and pressure. Carbon yield of pitches is better compared to thermosetting carbon precursors; accordingly, densification is completed faster. Since pitches are in the liquid form during processing, consolidation pressure around 20 bar has to be applied during carbonization to prevent bleeding of pitch [Sharma et al, 2017]. Impregnation and carbonization in high temperatures and pressures requires costly equipment.

Unlike carbon precursor based manufacturing, CVI method doesn't involve separate infiltration and carbonization stages. Hydrocarbon gases as methane, benzene, and propane are deposited to carbon fiber reinforced preform; then the gas is thermally decomposed to carbon on the heated surface of fiber preform around 1100 °C within inert environment [Sharma et al, 2017]. In addition to time consuming densifications, inhomogeneous densification could be observed as well because of the thermal gradient within fibrous preform. Therefore, the process has to be followed carefully, also could be interrupted to satisfy homogenous impregnation for both interior and exterior regions of

the preform [Peters, 1998]. CVD method provides stronger fiber-matrix interface than liquid phase carbon precursor infiltrations. Carbon matrix is formed just around reinforcement as the hydrocarbon decomposed on heated fibers [Heidenreich, 2015].

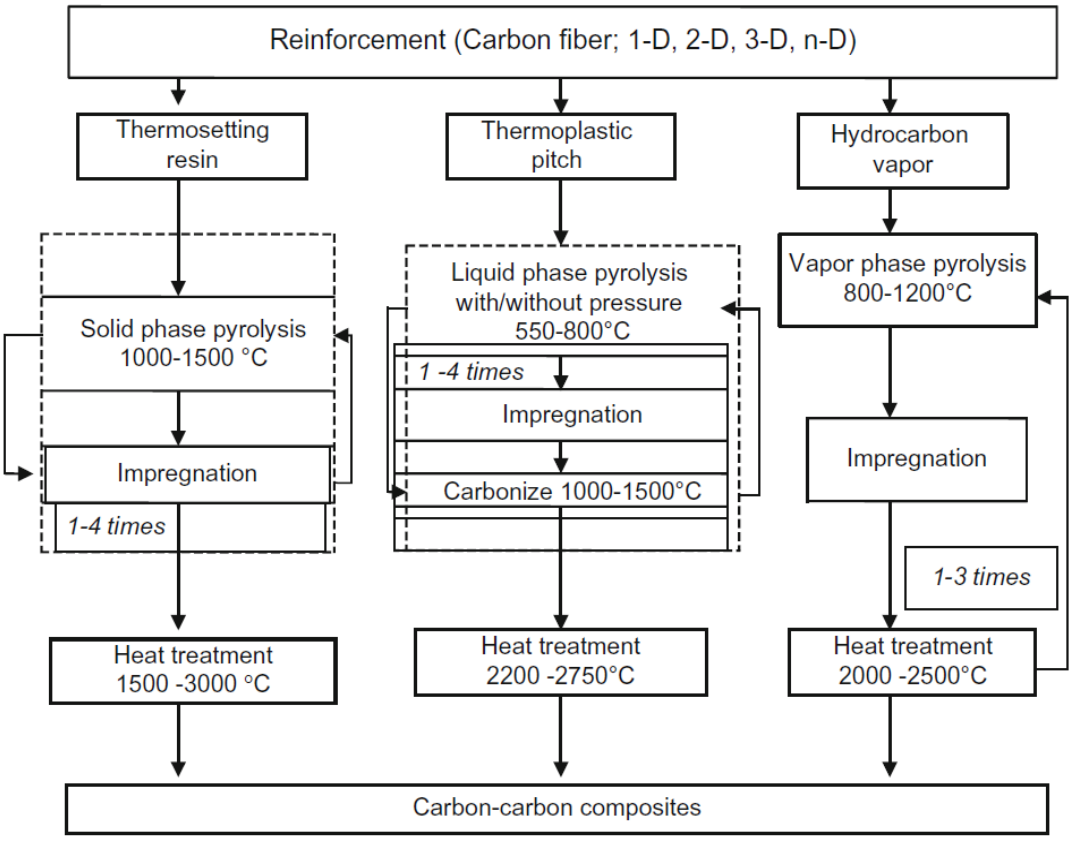

Figure 2.8: Processing Diagram of Carbon/Carbon Composites [Manocha, 2003]

C/Cs could be oxidized easily above 400°C. Low temperature oxidation prevents the potential use of C/Cs in high temperature load carrying applications. Two common approaches are available to protect C/Cs from oxidation; coating the surface by oxides, carbide, or nitrides; and modifying matrix by oxidation inhibitors such as boron (B), zirconium (Zr) and silicon (Si) [Chawla, 2012]. Silicon is widely preferred in inner and outer coatings of C/Cs, especially in nozzles of rockets and airbreathing engines. By embedding carbon fiber into partially or completely siliconized matrix, fibers could be protected against oxidation [Heidenreich, 2015]. Thus, carbon fiber could perform its high strength, stiffness, and fracture toughness behavior without exposing to oxidation.

2.2 Ablation Testing Methods

High temperature composite materials expose to various thermal, mechanical, and chemical effects depending on the application; accordingly materials have to be designed and tested. Even if it is impossible to test materials in exactly same conditions, especially in harsh rocket components; representative tests are conducted to simulate real applications. Total enthalpy, static pressure, Mach number, gas composition, and temperature would be close to actual application as much as possible. At least, dominating ablation mechanism could be sufficiently satisfied, in order to characterize selected materials. Arc-jet facilities are suitable for simulating re-entry flows by providing long duration, high enthalpy flows with helium (He), nitrogen (N_2), oxygen (O_2) gases. Gas composition could be arranged similar to atmosphere as well [Savino et al., 2018]. For radiative ablation tests, laser test facilities could produce very high heat flux for large size samples, but pressure and gas flow rate are low [Duffa, 2013]. Oxy-acetylene torch's flame could reach around 3000°C below 1 bar, also it is widely used because it is a cost-effective and standardized method [Rallini et al., 2019].

Rocket nozzles expose to thermo-chemically harsh and pressurized flow during the combustion. Especially in hybrid propellant rockets, oxidative hot gas reaches 2700°C around 15 to 35 bar static pressure with high flow rate. Long duration high temperature exposure could be satisfied by the stated facilities; however these setups generally couldn't provide high mass flux, pressurized chemically aggressive flow as the rocket application. By firing small scale rockets, representative firings tests could be configured to characterize nozzle materials. In the literature, lab-scale hybrid rocket motors were fired to test high temperature ceramic materials in the different locations of motors such as in the combustion chamber, the nozzle or placing the specimen away from nozzle exit [Mungiguerra et al., 2020]. Subscale solid rocket motors were used as well to assess ablative performance of insulator within the motor [Martin, 2013]. Small scale rocket firings exhibit low-cost and flight-like test for ablative materials.

Testing conditions have to be monitored in order to observe ablation conditions and estimate ablation rates. Aggressive thermo-chemical conditions are not suitable for using standard measurement instruments such as thermocouples and heat flux probes. These sensors could give fine measurements by direct contact with the source, but ablation test conditions are destructive for them. Infrared cameras and pyrometers are generally

preferred for high temperature testing measurements since they could obtain measurement without contact from the sample surface and heating source. Ablation conditions on the sample surface could be estimated by placing thermocouple and slug calorimeter to the backward as well. Depending on the surface boundary location, time, and thermal conductivity; surface temperature could be also estimated inversely, which requires intensive calculations and modelling [Martin, 2013] Moreover, the estimation model changes related to the ablation behavior such as melting and charring.

2.3 Hybrid Rocket Motors

Hybrid rockets are bipropellant chemical propulsion systems that store oxidizer in liquid or gaseous phase while storing the fuel in solid phase. Accordingly, they carry characteristics of both liquid and solid rockets. Oxidizer and fuel are stored in separate parts. During the firing, oxidizer is injected into fuel grain existing motor with valves. Ignition starts at the inlet of motor by the aid of igniter. After the igniter provides the required activation, oxidizer flow could be sustained and controlled during firing by controllable valves. Combustion occurs in the motor, and resultant products leaves the motor through the nozzle to provide thrust.

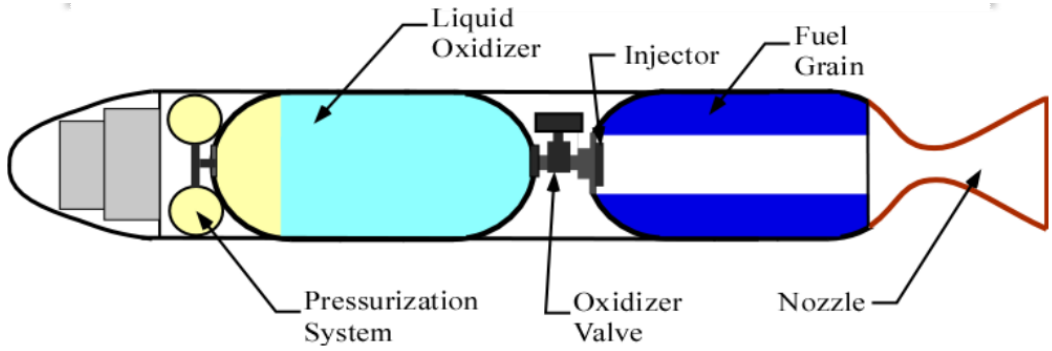

Figure 2.9: Hybrid Rochet Scheme [Karabeyoglu, 2023]

The oxidizer tank has to be pressurized for effective combustion. In order to pressurize combustion chamber with oxidizer, two common concepts are available, which are pressure tanks filled with inert gas to pressurize oxidizer tank or turbopump system feeding oxidizer to combustion chamber. Turbopump systems are superior in terms of weight and standard pressure feeding level, however it involves more sophisticated design

and material concept. Oxidizer tanks are heavier due to large volume of inert gas and pressure durable tank, also pressure drops (called blowdown) during the operation. Helium is preferrable as inert gas for the main launch system due to its low molecular weight.

Hybrid rockets are advantageous than liquid and solid concepts mainly in terms of safety, simplicity, and cost. Solid and liquid rockets have low tolerance to manufacturing errors. In hybrid propellant rockets, fuel is based on hydrocarbons which significantly lowers the explosion risk, also the combustion occurs within the fuel grain including motor and away from flammable oxidizer tank. Solid rocket fuels are very explosive, and liquid ones are more prone to catastrophic failures than hybrids. Additionally, hybrid rockets have throttling and stop-restart capability in spite of solid rockets. Hybrid rockets are also cost effective in terms of propellant selections and plumbing. Liquid systems have quite complex and costly subsystems [Altman et al., 2007]. In recent years, hybrid propulsion systems become popular solution for space mission operations, especially in satellite transfer systems [Lécossais et al., 2018].

2.3.1 Performance Parameters

Hybrid rocket propulsion is composed of multiple disciplines such as dynamics, solid mechanics, thermodynamics, and chemistry. According to terms related to these disciplines, propulsion systems are designed, and the performance of rockets are calculated. The rocket motor generates a thrust force by the combustion of propellants. Based on the amount of thrust, vehicle is accelerated or achieve a regular velocity [Sutton et al, 2017].

Thrust force F is integrated over firing time t, in order to obtain I_t which is total impulse applied on the vehicle.

$$I_t = \int_0^t F\, dt \tag{2.4}$$

Total impulse is proportional to energy obtained from the propellant. Propellant performances are generally compared without firing duration factor. Therefore, propellant combinations are assessed by considering their unit time thrust generations. Specific impulse I_{sp} refers to the thrust per unit propellant “weight” flow rate, which is

usually used to compare performances of different propellant selections [Sutton et al, 2017].

$$I_{sp} = \frac{\int_0^t F\, dt}{g_0 \int_0^t \dot{m}\, dt} \tag{2.5}$$

Firing conditions could be evaluated in total as well, then the formula simplifies to,

$$I_{sp} = \frac{I_t}{m_p . g_0} \tag{2.6}$$

where m_p indicates the total effective propellant mass that exits the motor. If thrust and propellant mass are assumed constant,

$$I_{sp} = \frac{F}{\dot{m} . g_0} = \frac{F}{\dot{w}} = \frac{I_t}{w} \tag{2.7}$$

The resultant products of combustion are ejected from the nozzle with high velocity. Thrust could be defined as the momentum change due to the exhaust gases with velocity v_e and mass flow rate $\dot{m}$.

$$F = \frac{d(m . v_e)}{dt} = \dot{w} . v_e \tag{2.8}$$

The equation 2.8 is valid if the exit pressure of nozzle equals to the ambient pressure, and it is called momentum thrust. The exit pressure could be more than the outside pressure. For example, the outside pressure varies during the flight because of the altitude change. If the nozzle exit pressure P_e is more than the ambient pressure P_a, that difference improves the thrust performance. The thrust factor added by this pressure difference is called pressure thrust [Sutton et al, 2017].

$$F = \dot{m} . v_e + (P_e - P_a) . A_e \tag{2.9}$$

The characteristic velocity c^*, is used to relatively estimate performances of propulsion systems. It is widely utilized in the chemical propulsion literature, also helpful

to compare relative performances of different propellant types and mixture ratios. By using the chamber pressure P_c, throat area A_t, and propellant mass flow rate $\dot{m}$; the characteristic velocity is calculated as below.

$$c^* = P_c A_t / \dot{m} \tag{2.10}$$

The thrust coefficient C_F is a dimensionless parameter to assess the performance and design quality of rocket motors. It is highly affected by the propellant gas property k, nozzle area A_t, nozzle exit area A_e, nozzle exit pressure P_e, ambient pressure P_a, and combustion chamber pressure P_c.

$$\begin{aligned} C_F &= \frac{T}{P_c A_t} \\ &= \sqrt{\frac{2k^2}{k-1}\left(\frac{2}{k+1}\right)^{(k+1)/(k-1)}\left[1-\left(\frac{P_e}{P_1}\right)^{(k-1)/k}\right]}\,\frac{P_e - P_a}{P_1}\frac{A_e}{A_t} \end{aligned} \tag{2.11}$$

Thrust coefficient C_F, specific impulse I_{sp} and characteristic velocity c^* could be combined in a single expression as well.

$$\begin{aligned} c^* &= I_{sp}\, g_0 / C_F \\ &= \frac{\sqrt{kRT_1}}{k\sqrt{[2/(k+1)]^{(k+1)/(k-1)}}} \end{aligned} \tag{2.12}$$

2.3.2 Interior Ballistics

The ballistic design of hybrid rockets begins with fuel and oxidizer selection. Most common fuel-oxidizer mixtures in hybrid propellants are LOX/Paraffin, LOX/HTPB, and N_2O(Nitrous Oxide)/Paraffin. Solid fuel geometries differ depending on missions, however single port grains are generally preferred because of repeatability and challenges in fuel grain manufacturing.

Hybrid motor characteristics largely relies on injector, nozzle, and chamber designs in addition to fuel combinations. Based on the mission and its requirements, optimum

fuel combination is selected for effective motor performance. The regression rate, Isp, and firing duration are critical parameters related to fuel selection of specific mission. After the fuel selection, optimum propellant mixture ratio is determined for efficient combustion. Optimum oxidizer to fuel mixture ratio (O/F) varies depending on the designed motor parameters since the optimum O/F varies based on chamber pressure and nozzle area ratio. The mixture ratio comprises both combusted and non-combusted propellants.

$$\frac{O}{F} = \frac{\dot{m}_{ox}}{\dot{m}_f} \tag{2.13}$$

The fuel grain of hybrid rockets does not include oxidizer. Since the fuel grain vaporizes before combustion, regression rate calculation has to contain radiative and convective heat transfer from flame that is zone near the boundary layer. Convective heat transfer is higher than the radiation of gas particles, therefore it takes part more in regression rate estimation. Diffusion limited regression rate model was derived accordingly, which was the result of convective heat transfer analyses in a turbulent boundary layer [Marxman et al., 1963].

$$\dot{r} = 0.036 \frac{G^{0.8}}{\rho_f} \left(\frac{\mu}{x}\right)^{0.2} \beta^{0.23} \tag{2.14}$$

In Equation 2.14, $\dot{r}$ represents the recession of fuel as per unit time, G is mass flow rate of propellant (oxidizer and fuel) per port area in the position of location x, ρ_f is fuel density in solid phase, μ indicates viscosity of combustion gas, and β is non-dimensional blowing parameter which involves contribution of vaporizing fuel on the fuel surface [Sutton et al, 2017].

The diffusion limited regression rate model still requires extensive tests to verify specific propellant systems. Also, the theoretical estimation of regression rate depends combined effects of pressure, grain length, mass flux and other design parameters. They are combined in propellant system as unique configuration, also there is not a direct proportionality within each other. Therefore, theory has to be supported by empirical derivations. The regression rate formula in below propose empirical derivations of

constants with more simplified form. Blowing coefficient β, location x, fuel density ρ_f, and combustion gas viscosity μ are merged in symbol α [Sutton et al, 2017]

$$\dot{r} = \alpha(G_0)^n \tag{2.15}$$

Instead of total propellant mass, G_0 represents oxidizer mass flux through the area of port A_p . Both α and n are empirical constants obtained by firing tests.

$$G_{ox} = \frac{\dot{m}_{ox}}{A_p} \tag{2.16}$$

In spite of cost and safety advantages of hybrid propellants rockets compared to solid and liquids, they have lower regression rate than both. Accordingly, comparatively low motor performance decreases the advantageous achievements of hybrid rockets. During the combustion, gasified fuel blows radially and blocks the heat transfer to fuel, which highly decreases the combustion efficiency. By using liquifying propellants such as paraffin and polyethylene waxes, liquid droplets are entrained and increases mass transfer mechanism during the combustion which contributes to effective combustion.

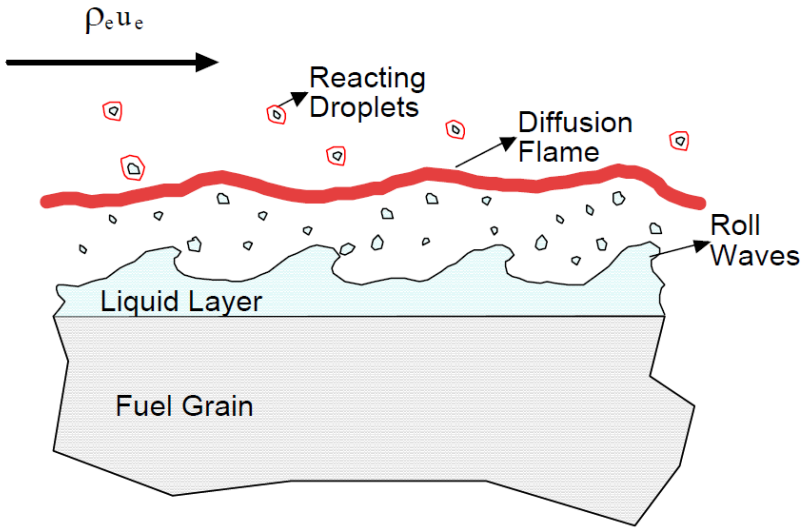

Figure 2.10: Entrainment Mechanism [Karabeyoglu et al. 2005]

Liquifying fuels could provide improved regression rate with entrainment mechanism. For example, paraffin-based fuels could burn up to four times more than conventional HTPB [Karabeyoglu et al. 2005]. Regression rate model constants of Equation 2.15 are stated below for different fuel combinations.

Table 2.3: Regression Rate Coefficients of Different Fuel-Oxidizer Combinations [Karabeyoglu, 2023]

Fuel – Oxidizer Combination	$\alpha\ [kg/(m^2.\text{sec})]$	n
$HTPB - LOX$	$3.043\ x\ 10^{-2}$	0.681
$HDPE - LOX$	$2.34\ x\ 10^{-2}$	0.62
$Paraffin - LOX$	$11.70\ x\ 10^{-2}$	0.62
$Paraffin - N_2O$	$15.50\ x\ 10^{-2}$	0.50

Chapter 3:
METHODOLOGY

In this study, phenolic and carbon matrix composite samples were tested under the free jet of hybrid rocket motor. Samples were manufactured in-house starting from the raw materials. Silica fabric reinforced, chopped silica fiber reinforced, and chopped carbon reinforced samples were manufactured with phenolic matrix. As carbon matrix composite samples; fabric and chopped fiber reinforced C/C samples were manufactured, also a batch of specified C/C samples were heat treated in 1500 °C. Due to common usage of graphite in rocket nozzle applications, graphite sample was also tested to consider as a reference material.

Prepared composite ablative samples were exposed to the hot gas of fuel and oxidizer rich hybrid propellant rocket motors. Since ablative composite materials are designed specific to applications; high temperature composite materials with different matrices, reinforcement types, and heat treatments were investigated for widely used propellant combination of hybrid rocket motors, which is paraffin - GOX.

3.1 Materials

3.1.1 Raw Materials

In this section, constituent raw materials of prepared samples is explained.

3.1.1.1 Phenolic Resin

In order to manufacture silica – phenolic composite with fabric reinforcement (SP-F) and carbon – carbon composite with fabric reinforcement (CC-F) samples, resol type phenol formaldehyde resin was preferred. It is single component resin system without hardener. The resin was commercially obtained. It contains 38 % isopropyl alcohol solvent by mass for increasing processibility, also the solid content of resin is 62%.

The carbon residue of phenolic resin after pyrolysis is critical for efficient C/C manufacturing, since the resin is also used for preparing fabric reinforced C/C precursors and densifying C/C samples. Selected resin leaves 64% carbon up to 900°C in the nitrogen atmosphere, which was observed by Thermogravimetric Analysis (TGA).

3.1.1.2 Novolac Powder

Phenol formaldehyde type hexamine hardener added novolac powder was used for manufacturing chopped fiber reinforced composite samples, which are silica – phenolic composite with chopped fiber reinforcement (SP-C), carbon – phenolic composite with chopped fiber reinforcement (CP-C), and carbon – carbon composite with chopped fiber reinforcement (CC-C). By mixing chopped fibers with dry powder resin, bulk molding compound was prepared for compression molding. Novolac powder contains hexamine hardener, also it does not lose considerable weight in curing stage.

Novolac type phenolic matrix composite is used as precursor in chopped fiber reinforced C/C manufacturing as well. Novolac powder leaves 60% carbon as result of pyrolysis, observed in TGA; which is critical for the precursor manufacturing of carbon – carbon composite with chopped fiber reinforcement (CC-C).

3.1.1.3 Carbon Fiber

Carbon fiber is used in carbon – phenolic composite with chopped fiber reinforcement (CP-C), carbon – carbon composite with chopped fiber reinforcement (CC-C), and carbon – carbon composite with fabric reinforcement (CC-F) samples. In CC-F composite samples, 12K 2x2 twill 660 gr/m^2 carbon fabric was used. Chopped carbon fiber strands are also 12K and they have 12mm length. Both chopped and fabric reinforcements are PAN based carbon fibers.

3.1.1.4 Silica Fiber

Silica fibers also are preferred in silica-phenolic with fabric reinforcement (SP-F) and silica-phenolic with chopped fiber reinforcement (SP-C) samples. Silica fabric has 612 gr/m^2, 8-harness satin weaving. Chopped silica fiber has 24 mm length strands. Silica fibers melt above 1650 °C.

3.1.1.5 Graphite

Graphite was obtained commercially. The grain size is 9 μm, and the ash content is 400 ppm. Additionally, it has 2760 °C service temperature in inert atmosphere.

3.1.2 Sample Preparation

By using raw materials stated in the previous section, samples were prepared for ablation tests. Specimens were extracted from the manufactured bulk materials, then machined into T-shape geometry in below.

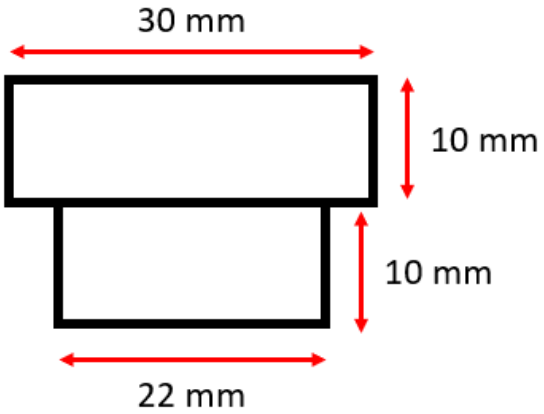

Figure 3.1: Dimensions of T-shape Samples

3.1.2.1 Phenolic Matrix Composites

Phenolic matrix based ablative samples can be classified in two groups in terms of reinforcement type; 2D fabric and chopped fiber reinforced polymeric composites. Fabric based samples are reinforced by silica, which are embedded in resol type phenolic matrix composites (SP-F: Silica Phenolic - Fabric Reinforced Samples). In the chopped fiber reinforced samples, silica and carbon strands were molded with novolac powder type phenolic matrix (SP-C: Silica Phenolic – Chopped Reinforced Samples, CP-C: Carbon Phenolic Chopped Fiber Reinforced Samples).

Silica fabric with 612 gr/m^2 8-harness satin weaving and carbon fabric with 660 gr/m^2 2x2 twill weaving were impregnated with resol type phenolic resin by brush. After stacking and impregnating sixty layers in the mold, impregnated layup was cured in hot press. Impregnated layup was dwelled in 80°C for 2 hours to get rid of IPA solvent, then ramped to 130°C with 1 °C/min and compressed with 5.5 MPa. After curing in 130°C for 3 hours, temperature was elevated to 150°C and held for 5 hours to be sure about complete curing (post curing). Due to the process was thick lamination curing, heating rates were low and dwell times were high. Cylindrical corks were extracted from the thick plates by waterjet, finally corks were machined by turning to sample geometry into the shape in

Figure 3.1. Carbon fabric reinforced phenolic matrix products were not tested but used for CC-F sample manufacturing.

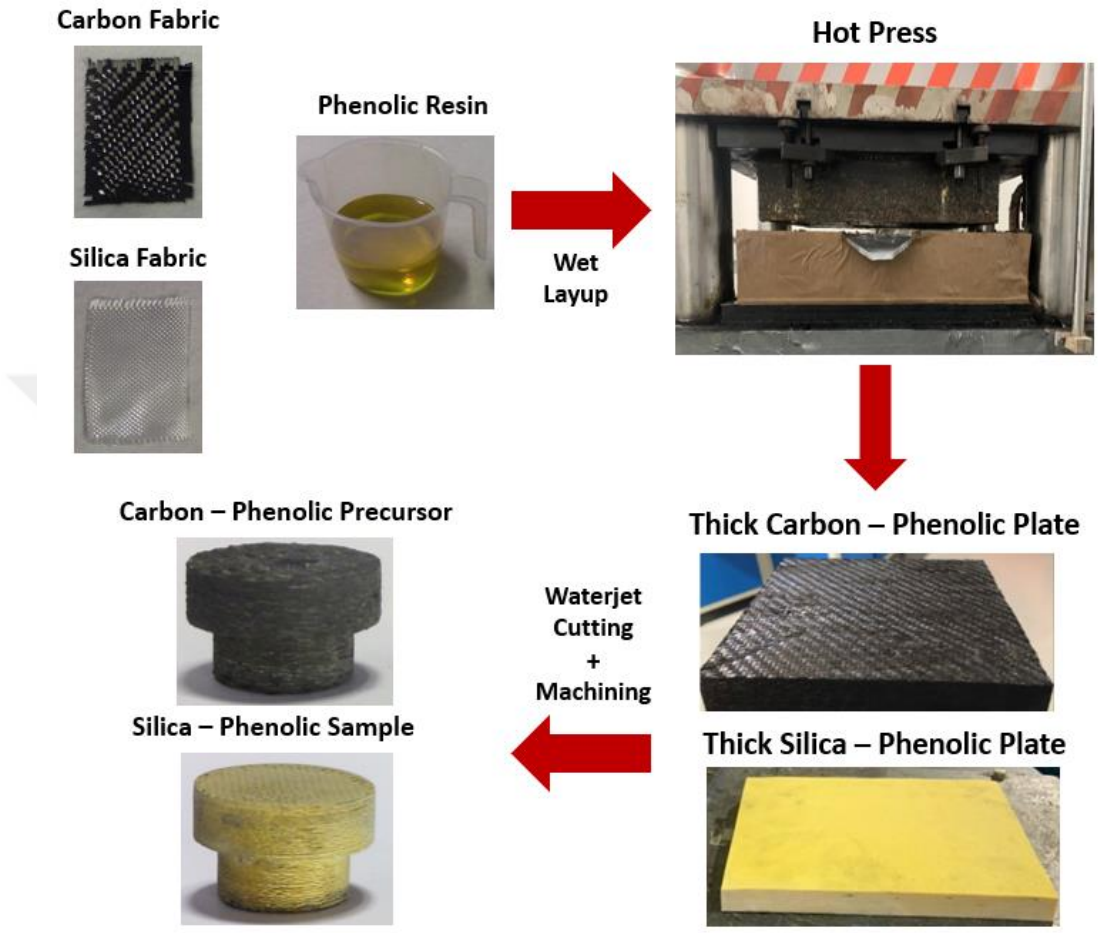

Figure 3.2: Manufacturing Schematic of Fabric Reinforced Phenolic Matrix Samples

Silica fiber strands with 24 mm length and carbon fiber strands with 12 mm length were mixed with novolac powder type phenolic resin to prepare bulk molding compound. Constituents were mixed in dry form by the stirrer rod, until obtaining homogenous mixture. Mixed molding compound was stacked and pressed in the mold. After stacking up finished, mold was heated to 80 °C and dwelled 1 hours. System should have homogenous temperature distribution before the curing reaction begins. Subsequently, molding compound was cured in 135 °C under 13.5 MPa. Demolded bulk part was cured in 150 °C for 5 hours again for post curing. Waterjet cutting and turning operations applied to bulk part for obtaining the sample geometry.

Figure 3.3: Manufacturing Schematic of Chopped Fiber Reinforced Phenolic Matrix Samples

The table below expresses density, total porosity, fiber, and resin volume fractions of phenolic matrix samples.

Table 3.1: Properties of Phenolic Matrix Samples

Sample Code	Density (gr/cm^3)	Total Porosity (%)	Fiber Volume Fraction (V_f)	Resin Volume Fraction (V_r)
SP-F	1.69 gr/cm^3	9.1 %	0.64	0.36
SP-C	1.63 gr/cm^3	3.6 %	0.46	0.54
CP-C	1.49 gr/cm^3	1.3 %	0.46	0.54

3.1.2.2 Carbon Matrix Composites

Hot pressed fabric reinforced carbon-phenolic and compression molded chopped reinforced carbon-phenolic polymeric matrix samples were utilized to manufacture C/C

samples. It was observed from the TGA data of resol and novolac type phenolic matrices that both resins complete mass loss until 900 °C in the pyrolysis. Therefore, these precursors were pyrolyzed in 900 °C. Pyrolysis occurred under nitrogen atmosphere with 1 °C/min ramp rate. During the pyrolysis, both types of samples lost 40% of their matrix weight. High mass loss rate could cause catastrophic cracks within the matrix or between fiber-matrix interface, so ramp rate was small in order to minimize deformation.

Pyrolyzed precursors converted to C/Cs having large void and low density after the first pyrolysis. Samples were densified by the re-infiltration of carbon matrix forming precursor , which was phenolic resin. By infiltrating phenolic resin into pores of C/C preforms, densities of samples were increased. C/C samples were placed in a container, then phenolic resin was infiltrated to container under vacuum. Vacuum level and process temperature are important to increase capillary effect for filling voids effectively. Phenolic infiltrated samples were cured in 130 °C for 3 hours, then samples were post-cured in 200 °C. Re-infiltration and pyrolysis cycles were repeated until the samples reached around 1.45 gr/cm^3 density and lower than 12% total porosity.

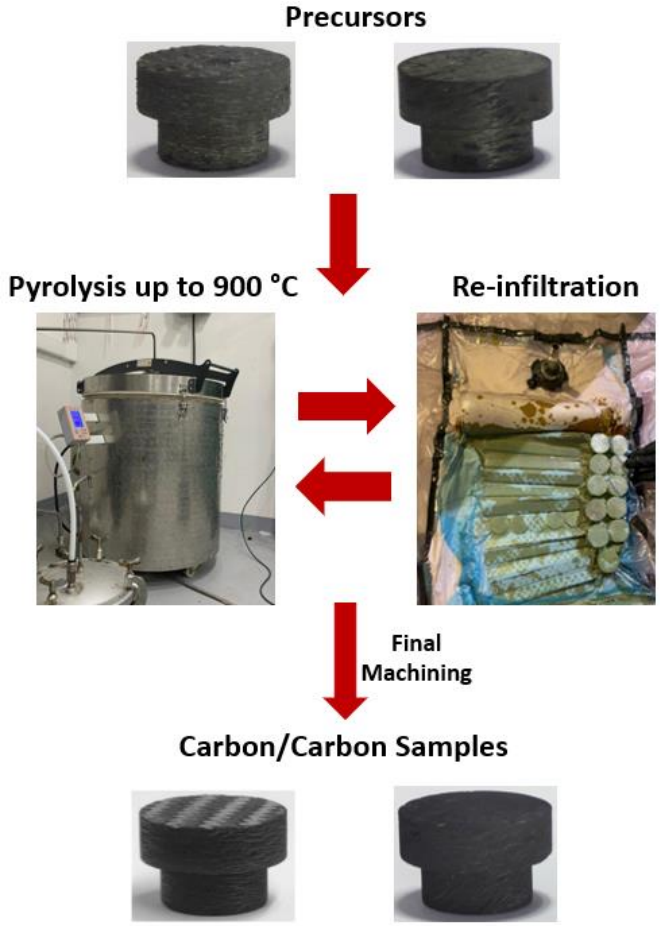

Figure 3.4: Carbon/Carbon Sample Manufacturing Schematics

After each densification, the void content of samples decreases by the formation of carbon matrix. In the meantime, some of open pores are blocked by newcomer matrix that causes conversion to closed pores. Densification efficiency decreases after each cycle, since pore channels start to close. The graph below shows density and open porosity content changes during the manufacturing stages.

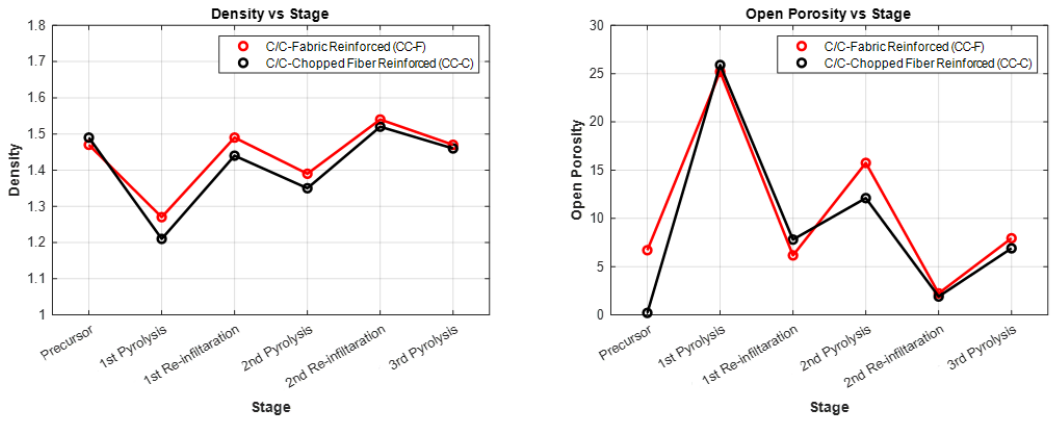

Figure 3.5: Densification Stages of C/C Samples: a) Density vs Stage, b) Open Porosity vs Stage

Normally, densification cycles could reach 6-8 times for larger parts, however it is easier to reach higher density in small parts due shorter and more interconnected pore channels. Two re-infiltration cycles were sufficient for the selected sample dimensions.

After reaching to desired density level, C/C parts could be heat treated in higher temperatures to develop high temperature stability. At elevated temperatures (1500 °C – 3000 °C), glassy carbon transforms into amorphous carbon by solid state transformation. Carbon microstructure becomes ordered and stabilized by the transformation. Accordingly, high temperature mechanical and thermal durability are increased [Muhammed, 2021]. In order to observe heat treatment effect on the ablative performance of C/C samples, a batch of fabric and chopped fiber reinforced samples were heat treated in 1500 °C after the 900°C pyrolysis. Therefore, heat treatment effect in the ablative performance of C/Cs were observed, specifically in hybrid rocket motor free jet case. Samples lost 2-3 % mass after the heat treatment that causes unremarkable decrease in the density and porosity.

Fabric and chopped fiber reinforced C/C samples with 1500 °C heat treatment are denoted as CC-F1500 and CC-C1500. Only 900 °C pyrolyzed C/C samples are labeled as CC-F900 and CC-C900. Some properties of C/C samples and graphite are shown in table below.

Table 3.2: Properties of C/C and Graphite Samples

Sample Code	Density (gr/cm^3)	Total Porosity (%)	Fiber Volume Fraction (V_f)	Resin Volume Fraction (V_r)
CC-F900	1.47 gr/cm^3	13.0 %	0.66	0.34
CC-F1500	1.44 gr/cm^3	15.6 %	0.67	0.33
CC-C900	1.46 gr/cm^3	11.0 %	0.50	0.50
CC-C1500	1.42 gr/cm^3	14.1 %	0.51	0.49
Graphite	1.83 gr/cm^3	8 %	-	-

Ablation rates are calculated from the difference between initial and final sample weights, since the ablation phenomena is directly related to heat dissipation of materials by sacrificing themselves. Basically, mass losses are divided into sample density, surface area and burn time.

$$\dot{s} = \frac{\frac{m_i - m_f}{\rho_{sample} . A_s}}{t_{burn}} \tag{3.1}$$

3.2 Experimental Setup

Prepared samples were tested under the free jet of paraffin fuel and GOX oxidizer lab scale hybrid rocket motor. The aim of tests is evaluating the performance of samples close to real hybrid motor firing conditions; hence the motor is designed by considering optimum performance.

The optimum O/F for paraffin - GOX hybrid motor is calculated from the NASA CEA. For the chamber pressure range 20 bar to 25 bar and 2.6 nozzle area ratio, optimum I_{sp} could be satisfied with 2.3 O/F.

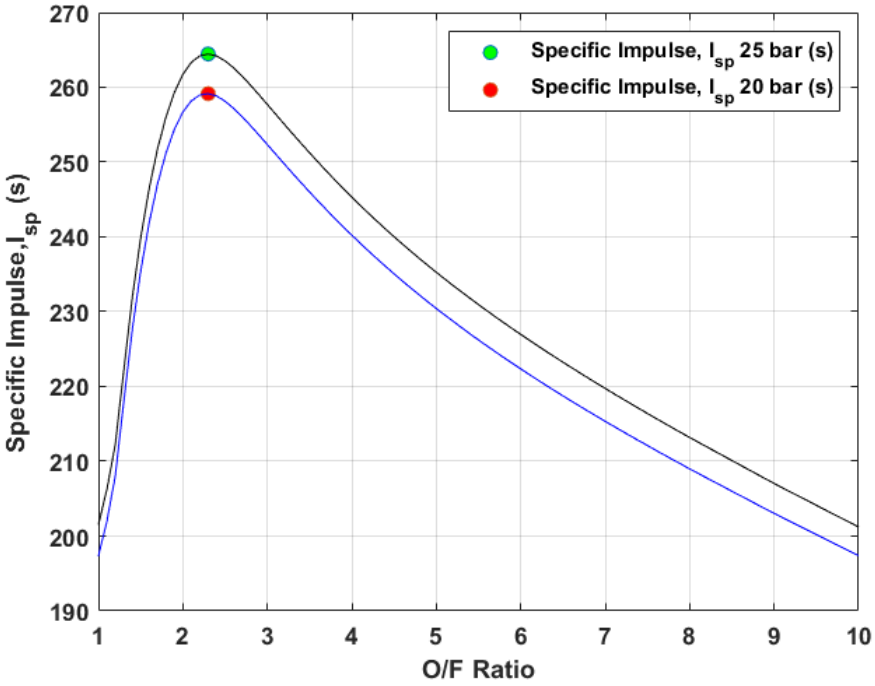

Figure 3.6: Optimal O/F for Paraffin - GOX Propellant Hybrid Motor

GOX injection was provided to pre-combustion chamber by 2.1 mm orifice which is connected to motor with port entrance. The cylindrical fuel grain had 65 mm outer diameter. After the fuel grain, post combustion chamber and nozzle were located. Graphite was used as nozzle material in firings.

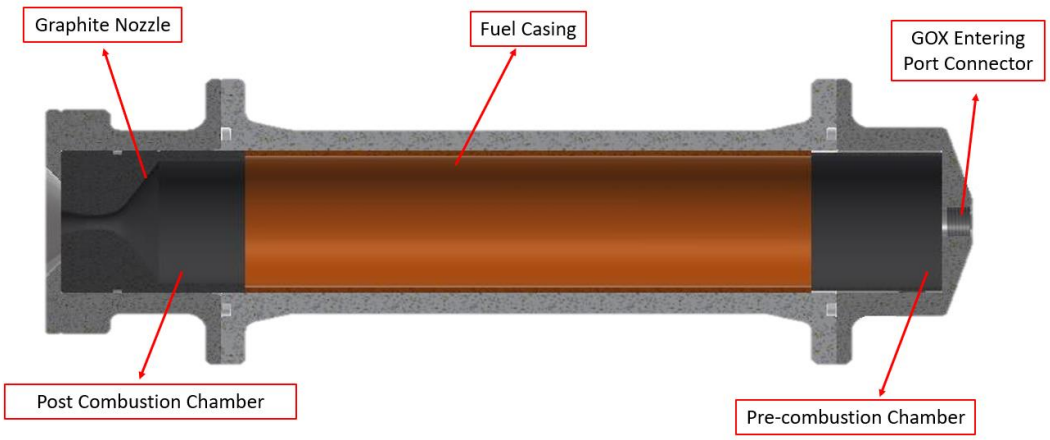

Figure 3.7: Hybrid Rocket Motor Schematic

Combustion temperature and products are highly O/F dependent factors (in addition to propulsion system design), also they are influential on the ablative material performances since combustion environment is deterministic in ablation mechanisms. Therefore, ablation rates of materials are in relation with O/F. Although the optimal O/F is 2.3, it will be better to test samples in fuel and oxygen rich firing cases in order to observe ablation performances in opposite extremes. It is expected that oxygen rich firing will propose high temperature oxidative firing environment, while fuel rich will form relatively low temperature with less oxidizing species.

Phenolic and carbon matrix samples were exposed to the free jet of motors with 2.6-2.8 and 2.1-2.2 O/F for 7 seconds duration. In order to eliminate mass flux effect on ablation and evaluate ablation performances based on O/F, the aim in motor design was determining oxygen and fuel rich firings with quite similar total mass flow rates. Similar total mass flow rate is satisfied with 23-24 bar combustion pressure in fuel rich motor and 25-26 bar in oxygen rich motor. The fuel length of fuel rich configuration was 250 mm, while oxidizer rich ones were 200 mm. CEA calculations show that oxygen rich motor has nearly 2675 °C nozzle exit temperature, while fuel rich motor has around 2275 °C and 2400 °C.

Table 3.3: Fuel and Oxidizer Rich Motor Configurations for Free Jet Tests

	Fuel Rich Motor	Oxygen Rich Motor
O/F	2.1-2.2	2.6-2.8
P_c	23 bar	25 bar
Fuel Length	250 mm	200 mm
$\dot{m}_{ox}$	49 g/sec	52 g/sec
$\dot{m}_{total}$	71-72 g/sec	71-73 g/sec
AR	2.6	2.6
t_b	7 second	7 second
T_e	2275-2400°C	2655-2675°C

The surface temperature of samples is detected by two-color pyrometer which measures temperature between 1000°C and 3000°C from a single point corresponding to

infrared radiation at 0.8–1.1 μm wavelengths. The surface temperature is determined from the ratio of two separate and overlapping infrared bands. Therefore, misdetection problem due to smoke and dust is eliminated, that is surface temperature would be accurately measured. T-shape samples are placed into a graphite sample holder and 260 mm away from the nozzle exit. Test duration is limited with 7 seconds to flame misalignment due to nozzle erosion.

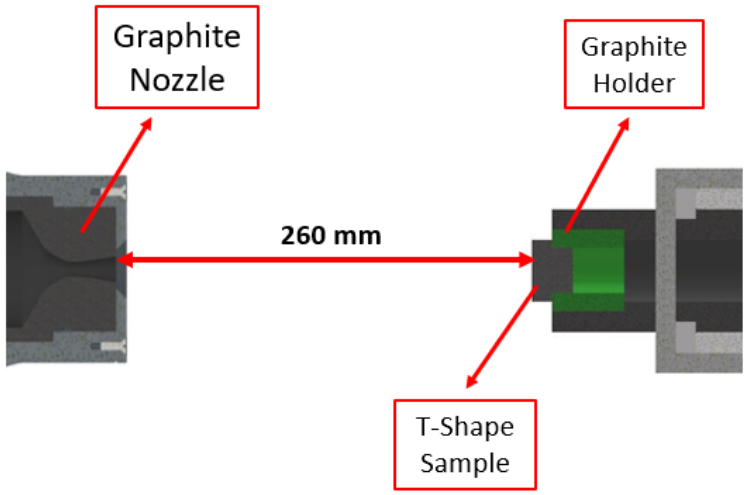

Figure 3.8: Free Jet Test Setup Schematic

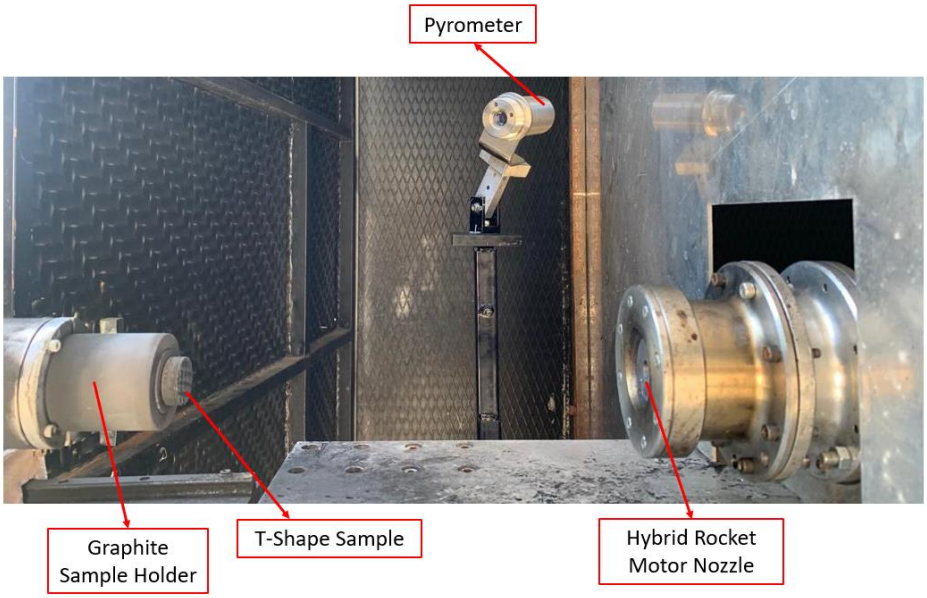

Figure 3.9: Free Jet Test Setup

In terms of sample labeling, fuel rich free jet tested samples are tagged with ‘FR’ abbreviation, likewise ‘OR’ tag is added for oxygen rich tests. For example, if the chopped silica fiber reinforced phenolic matrix sample is tested in fuel rich conditions, it will be denoted as SP-C-FR. For the same sample in oxygen rich condition, it will be called SiF-C-OR.

Chapter 4:
RESULTS & DISCUSSION

4.1 Results

4.1.1 Phenolic Matrix Composites Test Results

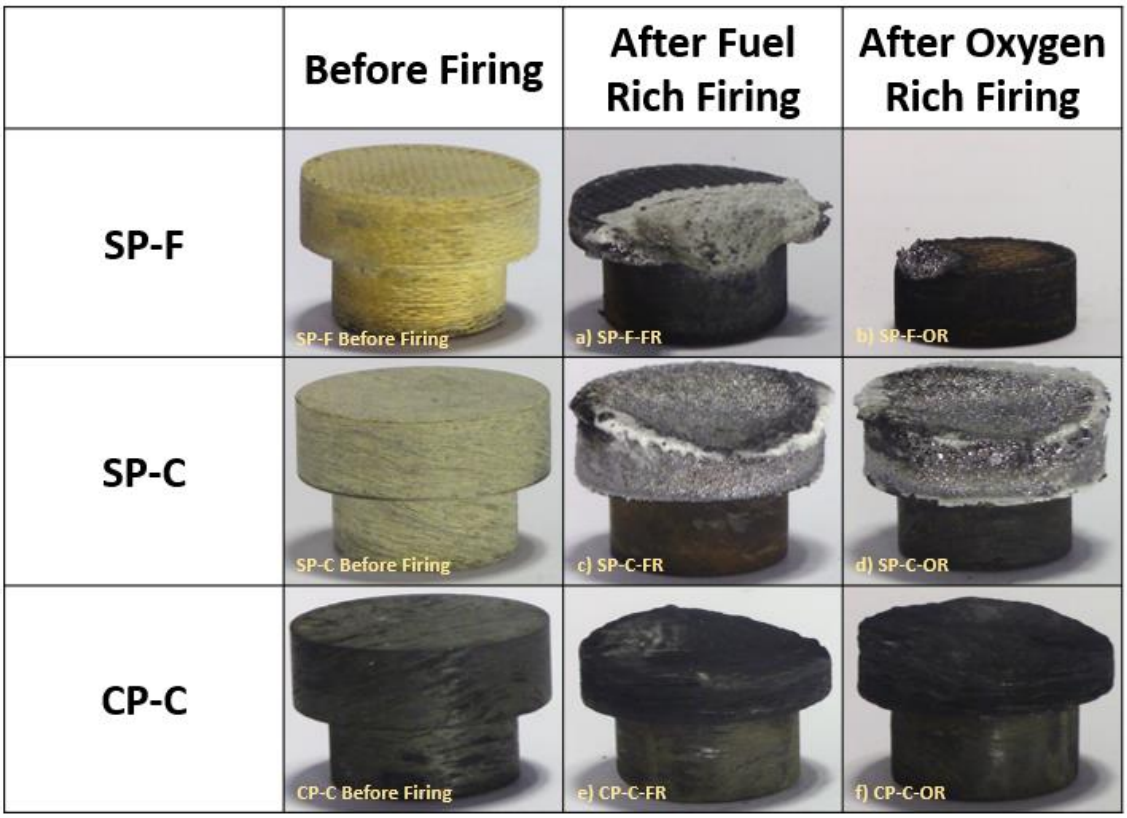

Figure 4.1: Appearance of Phenolic Matrix Composite Samples Before and After Tests: a) SP-F-FR, b) SP-F-OR, c) SP-C-FR, d) SP-C-OR, e) CP-C-FR, d) CP-C-OR

Silica fabric reinforced phenolic matrix samples performed considerably different ablation performance in fuel and oxygen rich firings. The large diameter section of SP-F-OR sample was completely ablated. SP-F-FR sample was delaminated as well; however it didn't as much as oxygen rich case. While SP-F-FR has localized silver colored melt silica region that shows the focus of hot gas, SP-F-OR has no indication of hot gas ablation and melt silica because of the severe delamination. In contrast to silica fabric reinforced samples, SP-C samples has similar surface appearance after both oxygen and

fuel rich firings. Surfaces of SP-C-FR and SP-C-OR samples were completely covered by melt silica that has bright silver color, also charred phenolic matrix emerged within the melt silica. Again, focus region of hot gas can be observed in deeper ablated region for SP-F samples. Surfaces of CP-C samples were exposed to mechanical spallation and resulted in wavy appearance, in both oxygen and fuel rich firings. Additionally, cracks were observed around the sample which were led by the pyrolysis of phenolic matrix. Rapid temperature increase causes uncontrolled gas release of pyrolyzing phenolic matrix; thus localized spallation on the surface and voids through the thickness had occurred.

The camera of pyrometer provided video during the firings that proposed clear vision to understand ablation mechanisms during tests. Even if the reinforcement-matrix combinations are highly deterministic in ablation mechanisms, the major ablation mechanism of samples were not remarkably varied based on the firing conditions, whether it was fuel or oxygen rich firing. Ablation testing of SP-F, SP-C, and CP-C samples are shown in Figure 4.2.

Figure 4.2: Images from the Tests of Phenolic Matrix Samples: a) SP-F, b) SP-C, and c) CP-C

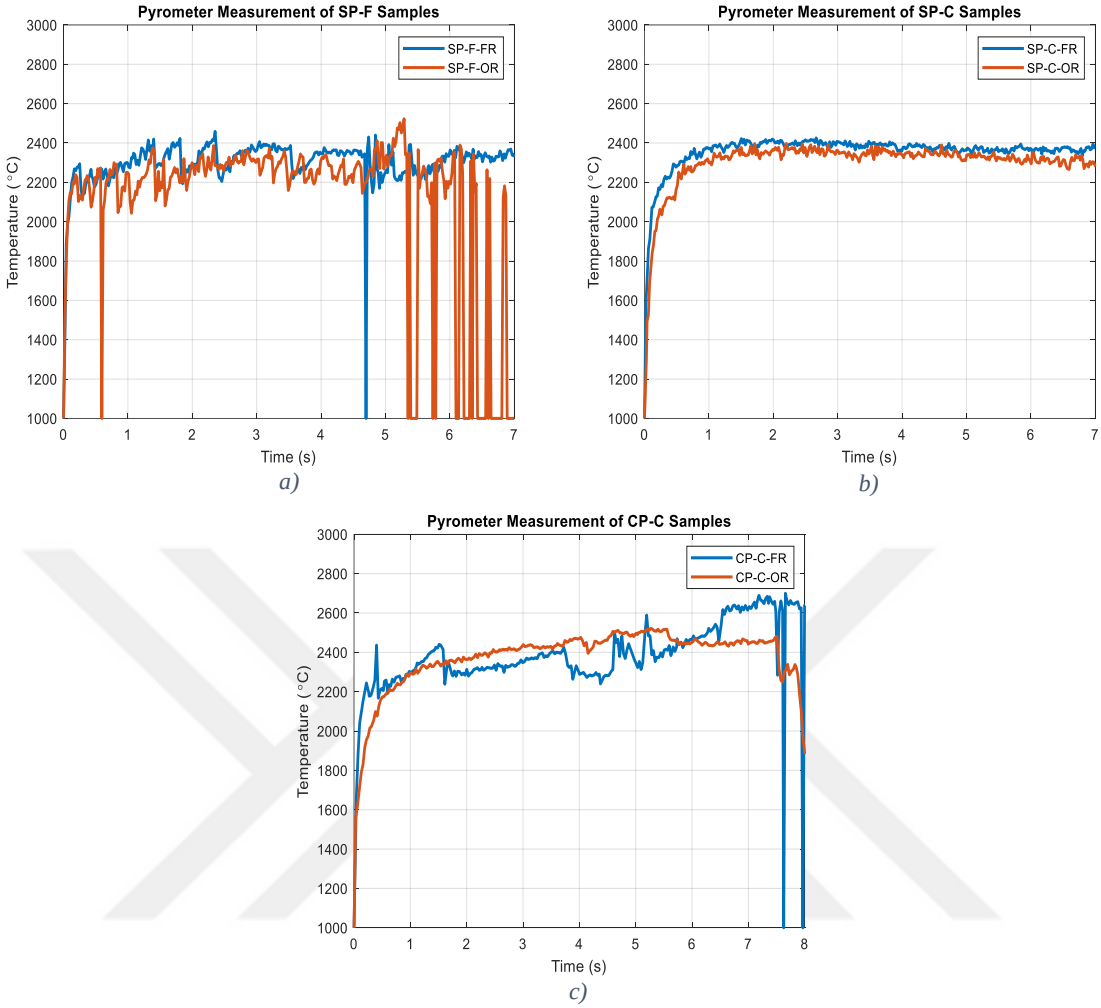

Figure 4.3 Pyrometer Measurements of Phenolic Matrix Samples:

SP-F, b) SP-C, and c) CP-C

SP-F ablation was mainly driven by the delamination of silica fabric layers, even if melting silica protected underlying layers from the hot gas during the test. As shown in Figure 4.2a, silica fabric concurrently melted and delaminated. There was no delamination in SP-C samples. As seen in Figure 4.2b, the surface of SP-C sample covered with melt silica layer. Silica droplets were also available around the periphery of large diameter. Due to the hot gas pressure on the surface, melt silica swept away from the surface. CF-Cs were oxidized from by the hot gas significantly, also separated pieces caused nonhomogeneous ablated surface.

Surface temperature of samples during tests are shown in Figure 4.3. Even if the surface temperature of SP-F samples were close to each other during the oxygen and fuel rich testing, SP-F-FR's temperature dropped fewer times compared to SP-F-OR which indicates delamination number. SP-F-OR had also noise-like sharp decreases, especially

towards the end of tests. These sudden decreases correspond to large sized fabric delamination, which were not removed from the graph intentionally to show harsh mechanical spallation mode in oxygen rich firings of SP-F samples.

SP-C-FR and SP-C-OR had similar surface temperature behavior, additionally there were no sudden temperature drops as fabric reinforced samples. While SP-C-FR was around 2400°C, SP-C-OR's surface temperature was between 2300°C to 2400°C.

CP-C samples had quite different surface temperature data. It was observed that CP-C-FR are exposed to sudden temperature drops due to localized fractures during the firing, however CP-C-OR had rather stable surface temperature with less fractures.

Table 4.1: Ablation Rates of Phenolic Matrix Samples

	Ablation Rate of Fuel Rich Firing (mm/sec)	Ablation Rate of Oxygen Rich Firing (mm/sec)
SP-F	0.939	2.832
SP-C	0.327	0.297
CP-C	0.861	0.610

Ablation rates of phenolic matrix samples are tabulated in Table 4.1, which were calculated based on Equation 3.1. Oxygen rich firing of SP-F sample ablated almost three times more than fuel rich ones, even if there were no considerable surface temperature level difference except delamination related temperature drops. SP-C had close ablation rates in fuel and oxygen rich firings; unlike silica-phenolic samples with fabric reinforcement (SP-F). Additionally, chopped silica resisted considerably better against hot gas exposure with respect to fabrics. As observed in pyrometer measurement and appearance of samples after tests, CP-C-FR sample had more and bigger damage regions compared to CP-C-OR, accordingly, CP-C-FR had higher ablation rate.

As seen in Table 3.3, oxygen rich hybrid motor configuration has higher nozzle exit temperature in addition to its more oxidizing hot gas content compared to fuel rich configuration. Therefore, oxygen rich firing induced more delamination of silica fabric layers in SP-F-OR compared to fuel rich tested SP-F-FR. More oxidizing hot gas

diffusion through the fabric layers might have caused the sudden gas release of pyrolyzing phenolic matrix, which caused debonding of fabric-matrix contact. In spite of the higher hot gas temperature of oxygen rich motor configuration, surface temperature of SP-F-FR and SP-F-OR were similar.

Although constituents of SP-F and SP-C are similar, SP-C samples performed similar ablation rates in both fuel and oxygen rich firings in contrast to SP-Fs. It seems that chopped silica within phenolic matrix provides better protection of phenolic matrix, by forming melt layer on the surface during the firings.

Despite of the higher oxidation potential of oxidizer rich firings, chopped carbon fiber reinforced phenolic sample CP-C ablated more in the fuel rich firings. Moreover, the surface temperature of CP-C-FR sometimes exceeded CP-C-OR. It might be related with fuel rich fired motor couldn't combust the fuel properly, that is, exiting hot gas could be still combusting non-combusted paraffin fuel in the outside of motor. Combustion can still continue to occur on the surface of ablation samples. SP-C sample of fuel rich firing had slightly higher temperature than the oxygen rich firing as well, that might also be related to ongoing combustion on the sample surfaces. Nevertheless, the chopped silica reinforced sample is affected less than the chopped carbon reinforced sample from the ongoing combustion.

4.1.2 Carbon Matrix Composites and Graphite Test Results

Figure 4.4 Appearance of Carbon Matrix Composites and Graphite Samples Before and After Tests: a) CC-F900-FR, b) CC-F900-OR, c) CC-F1500-FR, d) CC-F-1500-OR, e) CC-C900-FR, f) CC-C900-OR, g) CC-C1500-FR, h) CC-C1500-OR, i) Graphite-FR, j) Graphite-OR

Fired hybrid motor configuration is significantly influential in the ablation performance of CC-F900 samples. As shown in Figure 4.4, the carbon matrix of CC-

F900-OR was highly degraded compared to CC-F900-FR. In addition to upmost fabric layer, carbon matrix between the underlying layers was also degraded. Upmost fabric layer was partially broken and locally debonded from the carbon matrix. CC-F900-FR is in better situation with still bonded upmost fabric layer, also underneath layers are still relatively filled more with carbon matrix compared to CC-F900-OR. 1500°C heat treatment enhances the oxidation resistance of carbon matrix. The matrix of CC-F1500-OR sample seems degraded more compared to CC-F1500-FR sample, as in 900°C heat treated samples. By the effect of heat treatment, CC-F1500-OR performed better than CC-F900-OR sample. While large fabric pieces were removed from the surface of CC-F900-OR during the test, CC-F1500-OR layers were eroded locally. That is, CC-F1500-OR sample eroded through the thickness based on the focus of hot gas, rather than delamination of layers due to matrix oxidization as in CC-F900-OR. Bundles around the focus of hot gas remained intact in CC-F1500-OR. The matrix of CC-F1500-FR resisted better than CC-F900-FR as well. Because of the bundle breakage of CC-F900-FR, surface appeared flatter. In the CC-F1500-FR, carbon matrix beneath the upmost fabric layer is still bonded, and the sample was exposed to intra-bundle carbon matrix damages rather than interlayer damages.

Chopped fiber reinforced C/C samples behave quite different from fabric reinforced samples in fuel and oxygen rich firings. As illustrated in Figure 4.4, CC-C900-FR sample has dumpy wavy because of the mechanical spallation of relatively large pieces during the firing. CC-C900-OR also has wavy surface, but detached pieces were smaller. After 1500°C heat treatment of chopped reinforced carbon matrix samples, ablation resistances are improved. Mechanically damaged surface area of CC-C1500-FR sample is smaller with respect to CC-C900-FR sample. CC-C1500-OR has just a single cavity formed by hot gas focus; remaining surface is undamaged.

Graphite-FR and Graphite-OR both have a small cavity by the effect of hot gas. Mechanical spallation was not observed during these tests.

Figure 4.5: Images from the Tests of Carbon Matrix and Graphite Samples; a) CC-F, b) CC-C, and c) Graphite

CC-F samples are ablated mostly by bundle fractures and delamination, which was observed from the ablation test recordings. Firstly matrix is oxidized, then debonded fabric bundles and layers are detached from the ablation surface. CC-C samples have similar ablation behavior; however matrix oxidation causes local damages due to random oriented fiber reinforcement. Mechanical spallation behavior is not regular. Graphite is mainly oxidized, and there is no mechanical spallation on the surface.

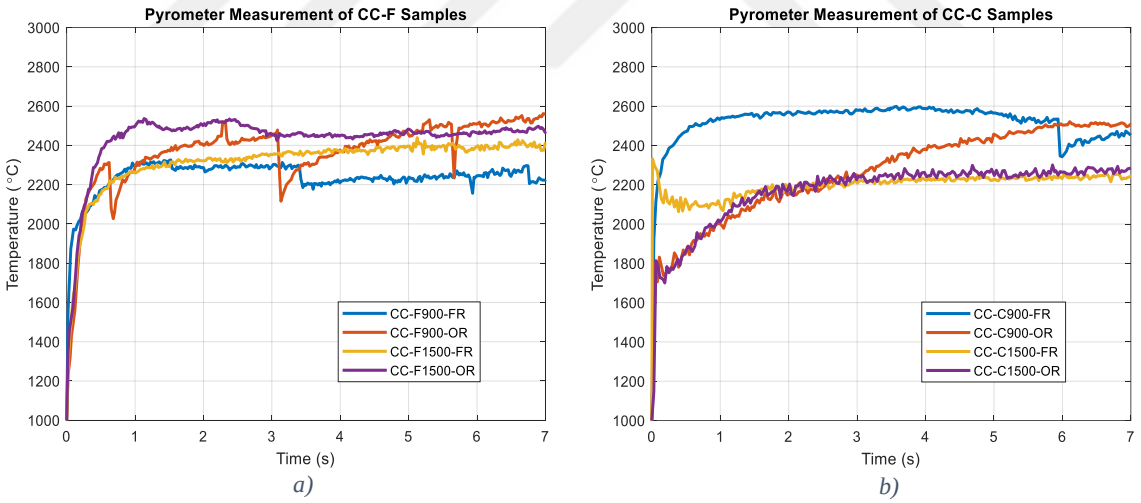

Figure 4.6: Pyrometer Measurements of Carbon Matrix Samples; a) CC-F, b) CC-C

CC-F900 samples were delaminated in both fuel and oxygen rich firings as shown in Figure 4.6a. Surface temperature of CC-F900-OR is higher than CC-F900-FR. Oxygen rich hot gas delaminated CC-F900-OR sample multiple times, which is observed from the number of sharp temperature declines. When it is compared with CC-F900-FR's sudden surface temperature decreases, the steeper decrease of CC-F900-OR's surface temperature can be interpreted as larger size of detached fabric. After the heat treatment

of fabric reinforced samples in 1500 °C, temperature trend of both CC-F1500-FR and CC-F1500-OR become steady and delamination failures are eliminated.

Despite the sudden temperature decreases of CC-F900-OR samples caused by delamination, the upper level of surface temperatures is quite similar in CC-F900-OR and CC-F1500-OR samples. CC-F900-OR's surface reaches to 2400-2500 °C range after each delamination, also the surface temperature of CC-F1500-OR is around 2400-2500 °C during the firing. In the case of fuel rich firings, CC-F900-FR and CC-F1500-OR samples have similar temperature magnitudes at the beginning, however CC-F900-FR's surface temperature decreases afterwards due to delamination. Consequently, the surface temperature ranges of samples are affected by more of firing configurations rather than the heat treatments.

Chopped fiber reinforced C/C samples, CC-Cs, performed quite different surface temperature behavior than CC-F samples. CC-C900-FR approaches to 2600 °C and stayed around here during the test, except a mechanical detachment of piece in the 6th second of the test. CC-C900-OR's surface temperature reaches to CC-C900-FR towards the end of test by ramping up until that time. Also it was observed that CC-C900 samples had higher surface temperature than CC-C1500 samples. The surface temperature of CC-C1500 samples is around 2200 °C, only CC-C1500-OR reaches to 2200 °C later than the CC-C1500-FR. It is clearly seen that 1500 °C heat treatment increases the conductivity of carbon matrix in chopped fiber reinforced samples; therefore surface temperatures are higher in 900 °C heat treated samples. Heat treatment improves the heat dissipation via conductivity.

Since graphite has high thermal conductivity and high heat capacity, it absorbed and transferred the heat rapidly during the tests. Pyrometer couldn't measure the surface temperature properly. Therefore, it measured the hot gas temperature and cold surface of graphite randomly, causing a noisy data. Thus, the surface temperature of graphite is not demonstrated.

Table 4.2: Ablation Rates of Carbon Matrix and Graphite Samples

	Ablation Rate of Fuel Rich Firing (mm/sec)	Ablation Rate of Oxygen Rich Firing (mm/sec)
CC-F900	0.375	0.502
CC-F1500	0.151	0.326
CC-C900	0.390	0.319
CC-C1500	0.213	0.157
Graphite	0.043	0.066

Fuel rich tested and 1500°C heat treated sample, CC-F1500-FR, performed better with respect to other fabric reinforced C/C samples, also CC-F900-OR sample ablated faster than others. It was observed that major part of ablation was caused by the delamination in fabric reinforced samples. Additionally, delamination occurs more in oxygen rich environment. Since the delamination phenomenon is based on debonding of fabric layers from the matrix, oxidation related matrix degradation is the main reason of ablation in fabric reinforced C/C samples. By applying heat treatment in 1500°C to samples; oxidation resistance and temperature resistance of carbon matrix are improved. Fiber-matrix bond is improved against high temperature environment; accordingly delamination is prevented in both fuel and oxygen rich firings. Although the carbon matrix is stabilized by the heat treatment, surface temperatures of fabric samples are still related to motor configuration of hybrid rocket motor. Oxygen rich firings cause higher surface temperature in both CC-F900 and CC-F1500 samples.

1500°C heat treated and oxygen rich tested sample resisted better in chopped carbon fiber reinforced samples. Although the oxidation potential and hot gas temperature of oxygen rich firings are higher, fuel rich fired samples were ablated more than oxygen rich fired samples in chopped carbon fiber reinforced carbon matrix samples. Surface temperatures of fuel rich tested samples increase faster than oxygen rich ones. The ablation of fuel rich tested samples might be advanced by the combustion of non-combusted paraffin fuel within the exited hot gas, which could increase the surface temperature of samples. While hot gas oxidizes the carbon matrix of fabric reinforced

samples by diffusing through the fabric; it can oxidize the matrix directly from the surface in chopped fiber reinforced samples. Essentially, the surface temperature of chopped fiber reinforced samples is deterministic in the oxidation of carbon matrix.

4.2 Discussion and Future Work

Phenolic and carbon matrix based composite samples were tested under the free jet of hybrid rocket with fuel and oxygen rich propellant mixtures. Among the phenolic matrix samples, silica-phenolic with chopped fiber reinforcement (SP-C) performed better ablation resistance than silica fabric reinforcement (SP-F) and chopped carbon reinforcement (CP-C). SP-C samples were steadily ablated by the formation of melt silica layer on the surface; therefore oxidation vulnerable phenolic matrix was exposed to oxidative hot gas with melt silica barrier. The constituents of SP-F samples are same with SP-C samples in terms of material types. However, the fabric layers of SP-Fs rapidly delaminated due to the sudden pyrolysis and oxidation of phenolic matrix, which led to debonding. Although CP-C samples have not layer-to-layer structure, the mechanical spallation of large pieces were observed by the sudden pyrolysis of phenolic matrix. SP-C samples propose better ablative solution than SP-F and CP-C against the thermochemically harsh free jet environment. Additionally, there was no considerable ablation rate difference between the fuel and oxygen rich firings of SP-C samples because of the silica's oxidation resistance and melting ablation behavior.

In the group of carbon matrix samples, carbon fabric reinforced (CC-F) and chopped carbon reinforced (CC-C) samples were tested. In addition to 900 °C pyrolyzed samples (CC-F900, CC-C900), a batch of samples were heat treated in 1500 °C (CC-F1500, CC-C1500) in order to improve thermal stability of carbon matrix. The root cause of CC-F ablation was delamination, but high temperature heat treatment improves the fiber-matrix bonding against ablation. Accordingly, CC-F1500 samples had remarkably better ablation resistance than CC-F900 samples in both fuel and oxygen rich firings. Even if CC-C samples has not layer-to-layer structure, 1500 °C heat treatment lowered ablation rates nearly to half of 900 °C pyrolyzed samples by lowering the mechanical spallation of CC/C pieces. That is, dominant ablation modes of C/C samples are delamination and mechanical spallation in both fabric and chopped fiber reinforced samples.

In oxygen rich firings, CC-Cs had nearly the half ablation rate of CC-F samples by the contribution of CC-Cs' increased thermal conductivity and nondirectional reinforcement structure. On the other hand, CC-F had lower ablation rate than CC-Cs in fuel rich firings. It is well known from the literature that fabric reinforced layer-to-layer stacks had significantly lower conductivity in the through thickness direction. Moreover, the oxidizer vulnerable matrix was probably protected from the direct free jet in fabric reinforced C/C samples, thanks to front fabric layer. The better ablation resistance of CC-F1500-FR than CC-C1500-FR can be explained with the barrier role fabric layer for matrix oxidation.

Among the phenolic matrix samples, best performing one was SP-C sample which had 0.327 mm/sec in the fuel rich firing and 0.297 mm/sec in the oxygen rich firing. For the carbon matrix samples, CC-F1500 had the lowest ablation rate 0.151 mm/sec in fuel rich firings, and CC-C1500 had 0.157 mm/sec. SP-Cs have non-homogenous ablation surface with its deep ablation damage, while CC-F1500 and CC-C1500 have rather flat surface. As expected, CMC class C/C samples outperformed in both fuel and oxygen rich firings, briefly they have almost twice better ablation rate than PMC class silica-phenolic with chopped fiber reinforcement. In addition to ablation rate difference, the ablation behavior of SP-Cs is not suitable for long-term firings as seen from the ablation damage on the sample surface. On the other hand, SP-C looks quite good solution among other PMC samples. It exhibits steady ablation trend with low mechanical failure risks in thermochemically harsh free jet environment.

Graphite had 0.043 mm/sec ablation rate in fuel firing and 0.066 mm/sec in oxygen rich firing. CC-F1500 was ablated with 0.151 mm/sec rate in fuel rich firing and CC-C1500 had 0.157 mm/sec in oxygen rich firing. Although the tested CMC and PMC samples are eligible for mechanical joining and have superior mechanical properties than graphite, additional processes are still required to reach graphite's ablation performance.

In future works, heat treatment above 1500 °C has to be applied to C/Cs in order to improve thermal stability and high temperature mechanical properties. Additionally, oxidation resistant matrices (such as silicon) and oxide coatings are applicable to C/C parts to develop ablation resistance. Composite based ablative materials have to be tested in long term firings, because materials might perform different behavior in long term firings. Thermocouple measurement can be obtained from the backend, through the long term firings, in order to observe the effect of thermal diffusivities on ablation

performance. Temperature measurements were obtained from the backend of sample surfaces in this study as well, however temperature trend couldn’t exhibit a certain trend due to the short time duration of firing.

Chapter 5:
CONCLUSION

The ablation performance of phenolic matrix and carbon matrix based composite materials are examined under the free jet of hybrid rocket motor in fuel and oxygen rich configurations. The ablation mechanisms of composite materials are explained according to the literature. Commonly used ablative composite materials and their critical manufacturing stages are investigated. After observing the testing conditions of ablative materials, a free jet test setup for the hybrid rocket motor case is implemented. Silica and carbon reinforced composite samples are tested in the setup.

Relying on the history of ablative materials; ablation mechanisms and limits of materials are defined. Ablative material processing is critically explored by considering the limits of industry and materials' tailoring structure. Polymer and ceramic matrix composites exhibit different ablative behavior as they include distinct material content and processing techniques. After presenting the available ablation testing methods in the literature, a test setup for hybrid rocket case is configured. The ablative materials within hybrid rocket motors are directly exposed to combustion conditions, therefore hybrid motor design and combustion outputs towards these materials are studied.

As the resin of polymer matrix composite, phenolic is selected by its prevalence; also silica and carbon reinforcements are combined with phenolic resin. In the class of ceramic matrix composites, C/C samples are obtained starting from the carbon-phenolic composites. Their manufacturing stages are explained by considering the material properties. Prepared samples are tested under the free jet of GOX-paraffin propellant hybrid rocket motor, in both fuel and oxidizer rich firing cases.

Test results show that chopped fiber reinforced silica-phenolic samples perform better ablation resistance among other phenolic matrix samples, in both fuel and oxidizer rich firing cases. In C/C samples, delamination and mechanical spallation problems are significantly lowered via 1500 °C heat treatment. Accordingly, 1500 °C heat treated fabric reinforced C/C sample has lowest ablation rate in fuel rich firings, also 1500 °C heat treated chopped reinforced C/C sample outperforms in oxygen rich firings. Additionally, best performing C/C samples have nearly twice lower ablation rates than chopped fiber reinforced silica-phenolic samples in both firing conditions.

In long term firings of hybrid rocket motors, the utilization of ceramic matrix composites looks inevitable because of their lightweight structure, considerable mechanical properties, and ablation resistance. Polymeric composites are preferrable in long term firings as well, but in the regions with less thermochemical and mechanical requirements. Even if C/C has lower ablation resistance than graphite in this study, the improvement of ablation resistance in C/Cs looks feasible by its tailoring manufacturing stages, such as improving fiber-matrix interface and higher temperature heat treatments. In addition to its designable manufacturing techniques; oxide coatings or oxidation resistant matrix development (such as silicon carbides) can be applied to C/Cs as well. Ultimately, C/Cs look critical material for the future of ablative materials.

BIBLIOGRAPHY

[Savino et al., 2017] Savino, R., Criscuolo, L., di Martino, G. D., Mungiguerra, S. (2018). Aero-thermo- chemical characterization of ultra-high-temperature ceramics for aerospace applications. Journal of the European Ceramic Society, 38(8), 2937–2953.

[Meetham et al., 2001] Meetham, G. W., Van de Voorde, M. H., Mishnaevsky, L., Jr. (2001). Materials for High Temperature Engineering Applications. Applied Mechanics Reviews, 54(5), B85-B85.

[Ariane-5, 2001] Ariane-5. (2001). http://www.arianespace.com

[Rallini et al., 2019] Rallini, M., Natali, M., Torre, L. (2019). An Introduction to Ablative Materials and High-Temperature Testing Protocols. In Nanomaterials in Rocket Propulsion Systems (pp. 529-549). Elsevier.

[Xiao et al., 2021] Xiao, J., Das, O., Mensah, R. A., Jiang, L., Xu, Q., Berto, F. (2021). Ablation Behavior Studies of Charring Materials with Different Thickness and Heat-flux Intensity. Case Studies in Thermal Engineering. 23.

[Schmidt, 1969] Schmidt, D. L. (1969). Ablative Polymers in Aerospace Technology. Journal of Macromolecular Science: Part A - Chemistry, 3(3), 327–365.

[Duffa, 2013] Duffa, G. (2013). Ablative Thermal Protection Systems Modeling. AIAA Education Series. American Institute of Aeronautics and Astronautics, Inc.

[Trick et al., 1997] Trick, K. A., Saliba, T. E., Sandhu, S. S. (1997). A kinetic model of the pyrolysis of phenolic resin in a carbon/phenolic composite. Carbon, 35(3), 393-401.

[Turchi, 2013] Turchi, A. (2013). A Gas-Surface Interaction Model for the Numerical Study of Rocket Nozzle Flows Over Pyrolyzing Ablative Materials. Doctoral dissertation, Universita degli Studi di Roma “La Sapienza”.

[Bradley et al., 1985] Bradley, D., Dixon-Lewis, G., din Habik, S. E., Mushi, E. (1985). The Oxidation of Graphite Powder in Flame Reaction Zones. Twentieth Symposium on Combustion, 20(1), 931-940.

[Natali et al., 2012] Natali, M., Torre, L. (2012). Composite materials: Ablative. Wiley encyclopedia of composites. Terni, Italy: University of Perugia.

[Favaloro, 2000] Favaloro, M. (2000). Ablative Materials. In Kirk-Othmer Encyclopedia of Chemical Technology. Wiley Blackwell.

[Martin, 2013] Martin, H. T. (2013). Assessment of the Performance of Ablative Insulators Under Realistic Solid Rocket Motor Operating Conditions. Doctoral dissertation, The Pennsylvania State University.

[Scala et al., 2013] Scala, S. M., Gilbert, L. M. (1965). Sublimation of graphite at hypersonic speeds. AIAA Journal, 3(9), 1635–1644.

[Turchi et al., 2019] Turchi, A., Paris, S., Walter Agostinelli, P., Grigat, F., Löhle, S., Bianchi, D., Ferracina, L. (2019). Assessment of the effect of heat-shield ablation on the aerodynamic performance of re-entry capsules in hypersonic flows. Proceedings of the 8th European Conference for Aeronautics and Aerospace Sciences (EUCASS).

[Onay, 2020] Onay, O. K. (2020). Ablation modeling for high-speed internal and external flows. Master's thesis, Middle East Technical University.

[Peters, 1998] Peters, S. T. (1998). Handbook of composites (2nd ed.). Chapman & Hall.

[Sharma et al, 2017] Sharma, S. D., Sowntharya, L., Kar, K. K. (2017). Polymer-Based Composite Structures: Processing and Applications. Composite Materials (1-36). Springer.

[Bansal et al., 2014] Bansal, N. P., Lamon, J. (2014). Ceramic Matrix Composites: Materials, Modeling, and Technology. Wiley.

[Chawla, 2012] Chawla, K. K. (2012). Composite Materials: Science and Engineering (3rd ed.). Springer.

[Rana et al., 2016] Rana, S., Fangueiro, R. (2016). Advanced Composite Materials for Aerospace Engineering: Processing, Properties and Applications (1st ed.). Woodhead Publishing.

[Coltelli et al., 2019] Coltelli, M. B. , Lazerri , A. (2019). Chemical Vapour Infiltration of Composites and Their Applications. In Chemical Vapour Deposition (CVD): Advances, Technology and Applications (pp. 363). CRC Press.

[Heidenreich, 2015] Heidenreich, B. (2015). C/SiC and C/C-SiC composites. In N. P. Bansal & J. Lamon (Eds.), Ceramic Matrix Composites: Materials, Modeling and Technology (1st ed., pp. 147–216). The American Ceramic Society, Wiley.

[Manocha, 2003], Manocha, L. M. (2003). High performance carbon-carbon composites. Sadhana, 28(1–2), 349.

[Savino et al., 2018], Savino, R., Criscuolo, L., di Martino, G. D., & Mungiguerra, S. (2018). Aero-thermo-chemical characterization of ultra-high-temperature ceramics for aerospace applications. Journal of the European Ceramic Society, 38(8), 2937–2953.

[Mungiguerra et al., 2020] Mungiguerra, S., di Martino, G. D., Savino, R., Zoli, L., Silvestroni, L., Sciti, D. (2020). Characterization of novel ceramic composites for rocket nozzles in high-temperature harsh environments. International Journal of Heat and Mass Transfer, 163

[Karabeyoglu, 2023] Karabeyoglu, A. (2019 (accessed December 27, 2023)). Hybrid Rocket Propulsion Fundamentals. https://web.stanford.edu/~cantwell/AA284A_Course_Material/Karabeyoglu AA 284A Lectures/AA284a_Lecture8.pdf

[Altman et al., 2007] Altman, D., & Holzman, A (2007). Overview and History of Hybrid Rocket Propulsion. In Fundamentals of Hybrid Rocket Combustion and Propulsion (pp. 1–36). American Institute of Aeronautics and Astronautics.

[Lécossais et al., 2018] Lécossais, A., Odic, K., Fiot, D., Lestrade, J.-Y., Verberne, O., et al. (2018). HYPROGEO Hybrid Propulsion: Latest project achievements. Space Propulsion 2018, Seville, Spain.

[Sutton et al, 2017] Sutton, G. P., Biblarz, O. (2017). Rocket Propulsion Elements. Wiley.

[Marxman et al., 1963] Marxman, G. and Gilbert, M. (1963). Turbulent Boundary Layer Combustion in the Hybrid Rocket. Vol 9.

[Karabeyoglu et al. 2005] Karabeyoglu, M. A., Cantwell, B. J., & Stevens, J. (2005, July). Evaluation of Homologous Series of Normal-Alkanes as Hybrid Rocket Fuels. 41st AIAA/ASME/ASEE Joint Propulsion Conference, Tucson, AZ.

[Karabeyoglu, 2023] Karabeyoglu, A. (2019 (accessed December 27, 2023)). Hybrid Rocket Propulsion Design Issues. https://web.stanford.edu/~cantwell/AA284A_Course_Material/Karabeyoglu%20AA%20284A%20Lectures/AA284a_Lecture10.pdf

[Muhammed, 2021] Muhammed, F., Lavaggi, T., Advani, S., Mirotznik, M., Gillespie, J. W. (2021). Influence of material and process parameters on microstructure evolution during the fabrication of carbon–carbon composites: A review. Journal of Materials Science, 56(32), 17877–17914.